

## Chapter 2

# Tectonics on a sphere: the geometry of plate tectonics

### 2.1 Plate tectonics

The Earth has a cool and therefore mechanically strong outermost shell called the *lithosphere* (Greek *lithos*, ‘rock’). The lithosphere is of the order of 100 km thick and comprises the crust and uppermost mantle. It is thinnest in the oceanic regions and thicker in continental regions, where its base is poorly understood. The *asthenosphere* (Greek *asthenia*, ‘weak’ or ‘sick’) is that part of the mantle immediately beneath the lithosphere. The high temperature and pressure which exist at the depth of the asthenosphere cause its viscosity to be low enough to allow viscous flow to take place on a geological timescale (millions of years, not seconds!). If the Earth is viewed in purely mechanical terms, the mechanically strong lithosphere floats on the mechanically weak asthenosphere. Alternatively, if the Earth is viewed as a heat engine, the lithosphere is an outer skin, through which heat is lost by conduction, and the asthenosphere is an interior shell through which heat is transferred by convection (Section 7.1).

The basic concept of *plate tectonics* is that the lithosphere is divided into a small number of nearly rigid *plates* (like curved caps on a sphere), which are moving over the asthenosphere. Most of the deformation which results from the motion of the plates – such as stretching, folding or shearing – takes place along the edge, or boundary, of a plate. Deformation away from the boundary is not significant.

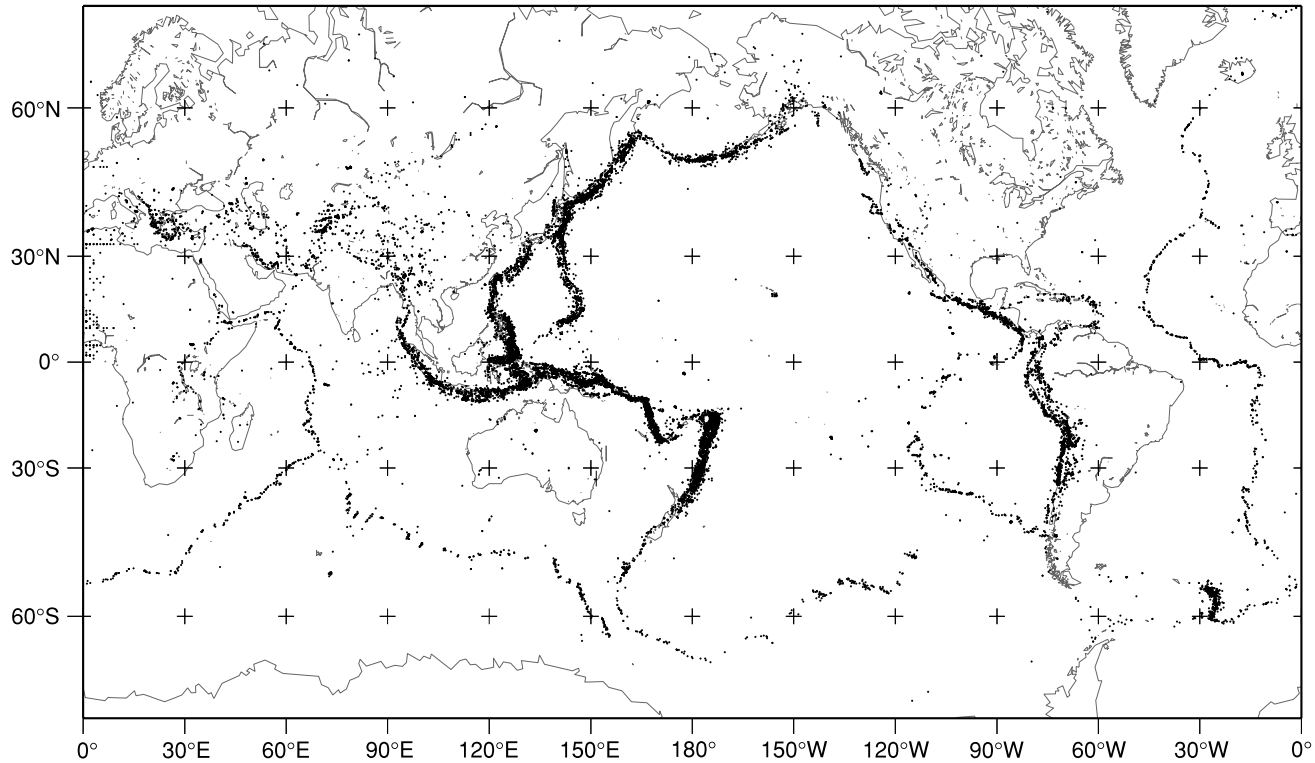
A map of the *seismicity* (earthquake activity) of the Earth (Fig. 2.1) outlines the plates very clearly because nearly all earthquakes, as well as most of the Earth’s volcanism, occur along the plate boundaries. These *seismic belts* are the zones in which differential movements between the nearly rigid plates occur. There are seven main plates, of which the largest is the Pacific plate, and numerous smaller plates such as Nazca, Cocos and Scotia plates (Fig. 2.2).

The theory of plate tectonics, which describes the interactions of the lithospheric plates and the consequences of these interactions, is based on several important assumptions.

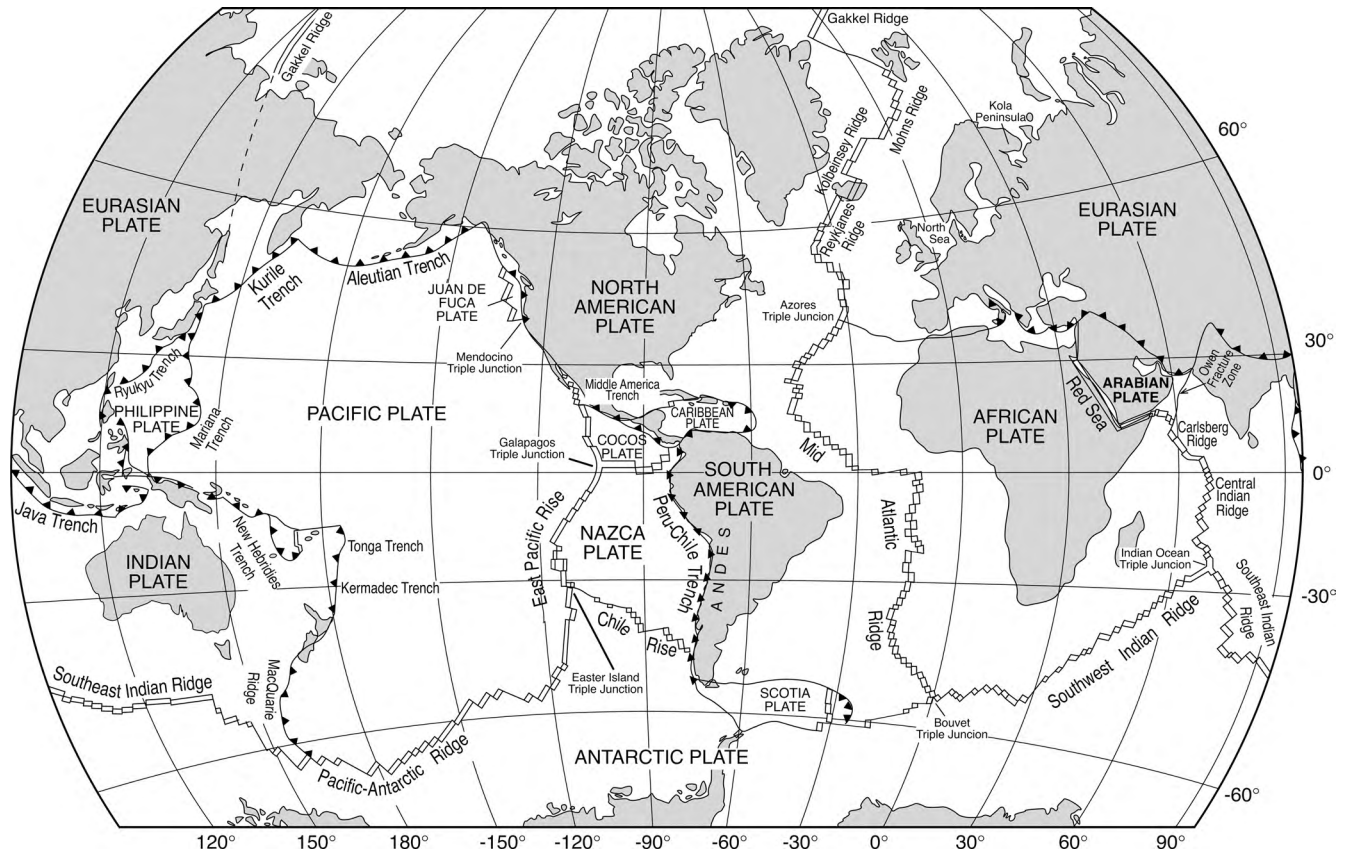
1. The generation of new plate material occurs by *seafloor spreading*; that is, new oceanic lithosphere is generated along the active mid-ocean ridges (see Chapters 3 and 9).
2. The new oceanic lithosphere, once created, forms part of a rigid plate; this plate may but need not include continental material.
3. The Earth's surface area remains constant; therefore the generation of new plate by seafloor spreading must be balanced by destruction of plate elsewhere.
4. The plates are capable of transmitting stresses over great horizontal distances without buckling, in other words, the relative motion between plates is taken up only along plate boundaries.

Plate boundaries are of three types.

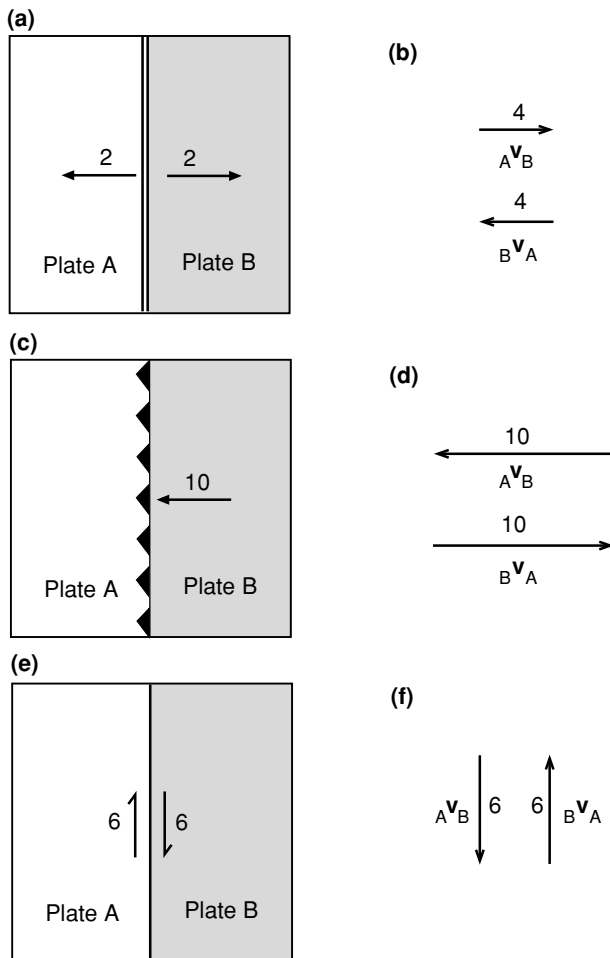
1. Along *divergent* boundaries, which are also called accreting or constructive, plates are moving away from each other. At such boundaries new plate material, derived from the mantle, is added to the lithosphere. The divergent plate boundary is represented by the *mid-ocean-ridge system*, along the axis of which new plate material is produced (Fig. 2.3(a)).
2. Along *convergent* boundaries, which are also called consuming or destructive, plates approach each other. Most such boundaries are represented by the *oceanic-trench, island-arc* systems of *subduction zones* where one of the colliding plates descends into the mantle and is destroyed (Fig. 2.3(c)). The downgoing plate often penetrates the mantle to depths of about 700 km. Some convergent boundaries occur on land. Japan, the Aleutians and the Himalayas are the surface expression of convergent plate boundaries.
3. Along *conservative* boundaries, lithosphere is neither created nor destroyed. The plates move laterally relative to each other (Fig. 2.3(e)). These plate boundaries are represented by *transform faults*, of which the San Andreas Fault in California, U.S.A. is a famous example. Transform faults can be grouped into six basic classes (Fig. 2.4). By far the most common type of transform fault is the ridge–ridge fault (Fig. 2.4(a)), which can range from a few kilometres to hundreds of kilometres in length. Some very long ridge–ridge faults occur in the Pacific, equatorial Atlantic and southern oceans (see Fig. 2.2, which shows the present plate boundaries, and Table 8.3). Adjacent plates move relative to each other at rates up to about  $15 \text{ cm yr}^{-1}$ .



**Figure 2.1.** Twenty-three thousand earthquakes with magnitudes greater than 5.2 occurred between 1978 and 1989 at depths from 0 to 700 km. These earthquakes clearly delineate the boundaries of the plates. (From ISC catalogue.)



**Figure 2.2.** The major tectonic plates, mid-ocean ridges, trenches and transform faults.



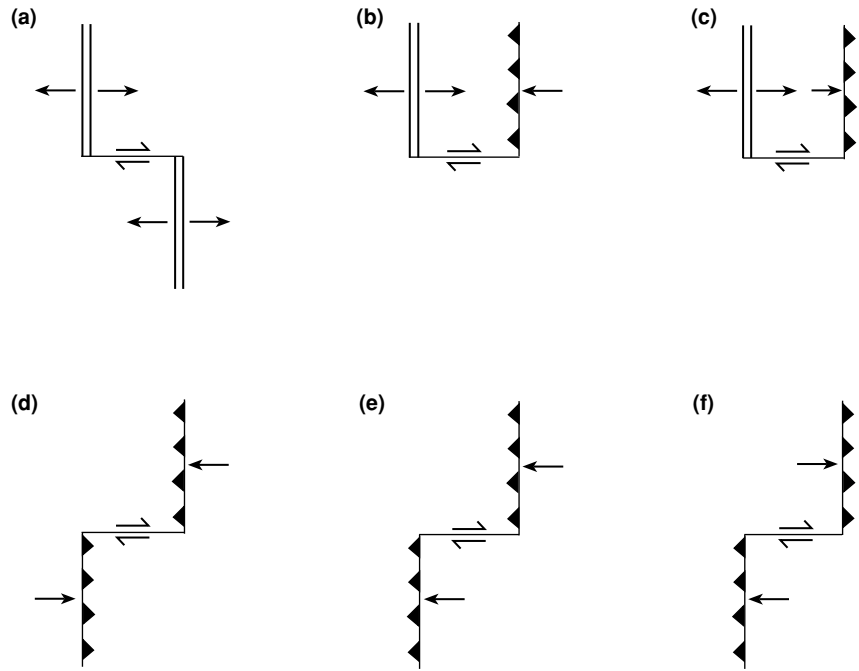
**Figure 2.3.** Three possible boundaries between plates A and B.

(a) A *constructive* boundary (mid-ocean ridge). The double line is the symbol for the ridge axis, and the arrows and numbers indicate the direction of spreading and relative movement of the plates away from the ridge. In this example the half-spreading rate of the ridge (half-rate) is  $2 \text{ cm yr}^{-1}$ ; that is, plates A and B are moving apart at  $4 \text{ cm yr}^{-1}$ , and each plate is growing at  $2 \text{ cm yr}^{-1}$ . (b) The relative velocities  ${}^A\mathbf{v}_B$  and  ${}^B\mathbf{v}_A$  for the ridge shown in (a).

(c) A *destructive* boundary (subduction zone). The barbed line is the symbol for a subduction zone; the barbs are on the side of the overriding plate, pointing away from the subducting or downgoing plate. The arrow and number indicate the direction and rate of relative motion between the two plates. In this example, plate B is being subducted at  $10 \text{ cm yr}^{-1}$ . (d) The relative velocities  ${}^A\mathbf{v}_B$  and  ${}^B\mathbf{v}_A$  for the subduction zone shown in (c).

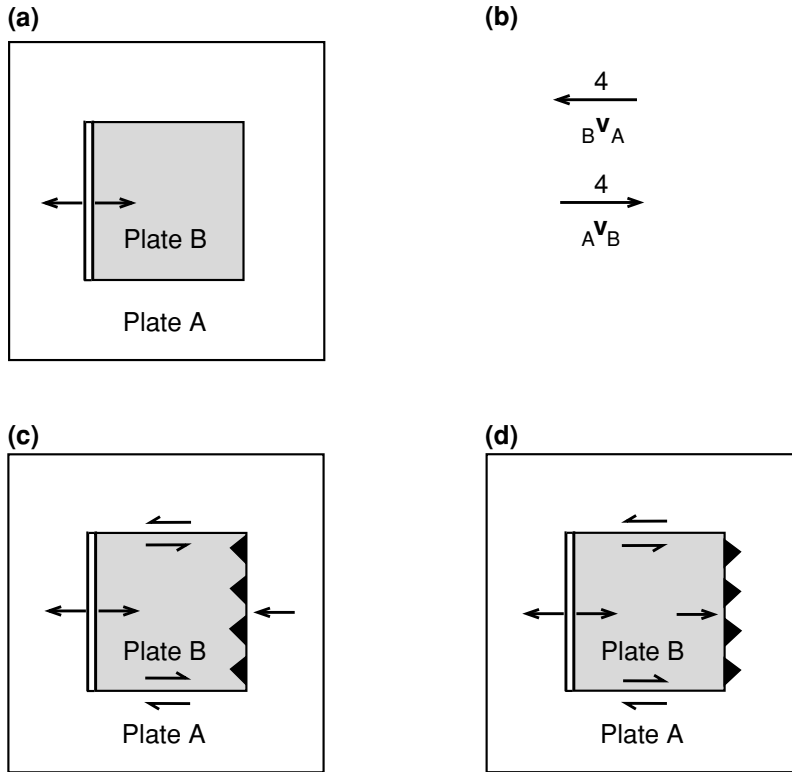
(e) A *conservative* boundary (transform fault). The single line is a symbol for a transform fault. The half-arrows and number indicate the direction and rate of relative motion between the plates: in this example,  $6 \text{ cm yr}^{-1}$ . (f) The relative velocities  ${}^A\mathbf{v}_B$  and  ${}^B\mathbf{v}_A$  for the transform fault shown in (e).

**Figure 2.4.** The six types of dextral (right-handed) transform faults. There are also six sinistral (left-handed) transform faults, mirror images of those shown here. (a) Ridge–ridge fault, (b) and (c) ridge–subduction-zone fault, (d), (e) and (f) subduction-zone–subduction-zone fault. (After Wilson (1965).)



The present-day rates of movement for all the main plates are discussed in Section 2.4.

Although the plates are made up of both oceanic and continental material, usually only the oceanic part of any plate is created or destroyed. Obviously, seafloor spreading at a mid-ocean ridge produces only oceanic lithosphere, but it is hard to understand why continental material usually is not destroyed at convergent plate boundaries. At subduction zones, where continental and oceanic materials meet, it is the oceanic plate which is subducted (and thereby destroyed). It is probable that, if the thick, relatively low-density continental material (the continental crustal density is approximately  $2.8 \times 10^3 \text{ kg m}^{-3}$ ) reaches a subduction zone, it may descend a short way, but, because the mantle density is so much greater (approximately  $3.3 \times 10^3 \text{ kg m}^{-3}$ ), the downwards motion does not continue. Instead, the subduction zone ceases to operate at that place and moves to a more favourable location. Mountains are built (*orogeny*) above subduction zones as a result of continental collisions. In other words, the continents are rafts of lighter material, which remain on the surface while the denser oceanic lithosphere is subducted beneath either oceanic or continental lithosphere. The discovery that plates can include both continental and oceanic parts, but that only the oceanic parts are created or destroyed, removed the main objection to the theory of *continental drift*, which was the unlikely concept that somehow continents were ploughing through oceanic rocks.



**Figure 2.5.** (a) A two-plate model on a flat planet. Plate B is shaded. The western boundary of plate B is a ridge from which seafloor spreads at a half-rate of  $2 \text{ cm yr}^{-1}$ . (b) Relative velocity vectors  ${}_A \mathbf{v}_B$  and  ${}_B \mathbf{v}_A$  for the plates in (a). (c) One solution to the model shown in (a): the northern and southern boundaries of plate B are transform faults, and the eastern boundary is a subduction zone with plate B overriding plate A. (d) An alternative solution for the model in (a): the northern and southern boundaries of plate B are transform faults, and the eastern boundary is a subduction zone with plate A overriding plate B.

## 2.2 A flat Earth

Before looking in detail at the motions of plates on the surface of the Earth (which of necessity involves some spherical geometry), it is instructive to return briefly to the Middle Ages so that we can consider a flat planet.

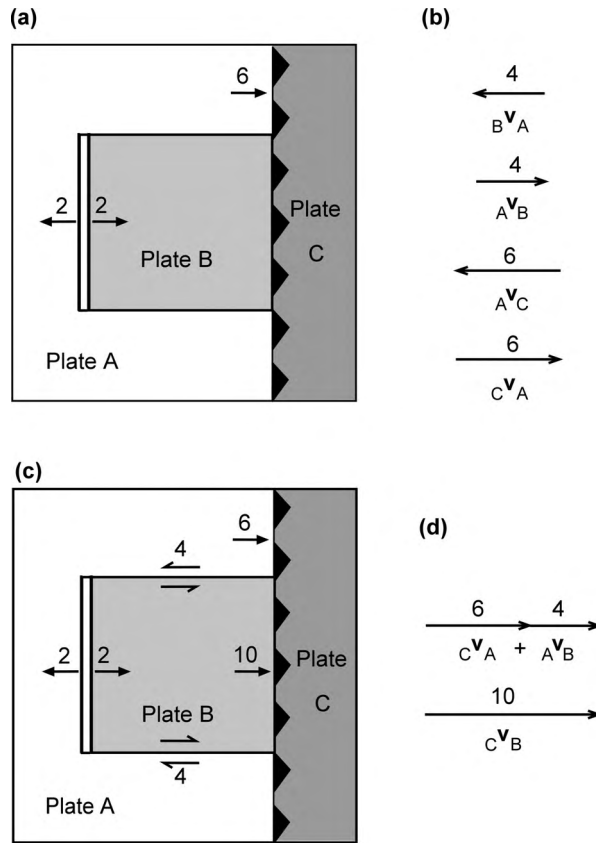
Figure 2.3 shows the three types of plate boundary and the ways they are usually depicted on maps. To describe the relative motion between the two plates A and B, we must use a vector that expresses their relative rate of movement (relative velocity). The velocity of plate A with respect to plate B is written  ${}_B \mathbf{v}_A$  (i.e., if you are an observer on plate B, then  ${}_B \mathbf{v}_A$  is the velocity at which you see plate A moving). Conversely, the velocity of plate B with respect to plate A is  ${}_A \mathbf{v}_B$ , and

$${}_A \mathbf{v}_B = -{}_B \mathbf{v}_A \quad (2.1)$$

Figure 2.3 illustrates these vectors for the three types of plate boundary.

To make our models more realistic, let us set up a two-plate system (Fig. 2.5(a)) and try to determine the more complex motions. The western boundary of plate B is a ridge that is spreading with a half-rate of  $2 \text{ cm yr}^{-1}$ . This information enables us to draw  ${}_A \mathbf{v}_B$  and  ${}_B \mathbf{v}_A$  (Fig. 2.5(b)). Since we know the

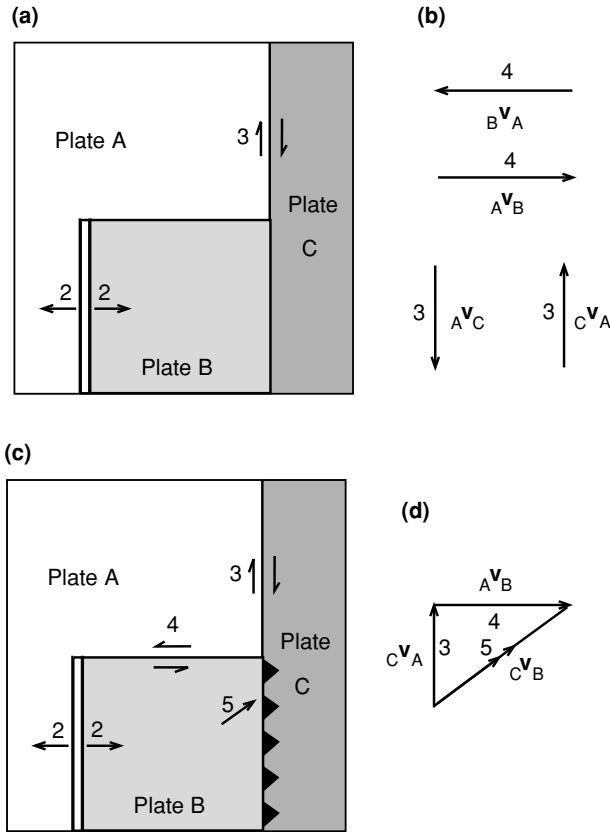
**Figure 2.6.** (a) A three-plate model on a flat planet. Plate A is unshaded. The western boundary of plate B is a ridge spreading at a half-rate of  $2 \text{ cm yr}^{-1}$ . The boundary between plates A and C is a subduction zone with plate C overriding plate A at  $6 \text{ cm yr}^{-1}$ . (b) Relative velocity vectors for the plates shown in (a). (c) The solution to the model in (a): the northern and southern boundaries of plate B are transform faults, and the eastern boundary is a subduction zone with plate C overriding plate B at  $10 \text{ cm yr}^{-1}$ . (d) Vector addition to determine the velocity of plate B with respect to plate C,  ${}_C\mathbf{v}_B$ .



shape of plate B, we can see that its northern and southern boundaries must be transform faults. The northern boundary is *sinistral*, or left-handed; rocks are offset to the left as you cross the fault. The southern boundary is *dextral*, or right-handed; rocks are offset to the right as you cross the fault. The eastern boundary is ambiguous:  ${}_A\mathbf{v}_B$  indicates that plate B is approaching plate A at  $4 \text{ cm yr}^{-1}$  along this boundary, which means that a subduction zone is operating there; but there is no indication as to which plate is being subducted. The two possible solutions for this model are shown in Figs. 2.5(c) and (d). Figure 2.5(c) shows plate A being subducted beneath plate B at  $4 \text{ cm yr}^{-1}$ . This means that plate B is increasing in width by  $2 \text{ cm yr}^{-1}$ , this being the rate at which new plate is formed at the ridge axis. Figure 2.5(d) shows plate B being subducted beneath plate A at  $4 \text{ cm yr}^{-1}$ , faster than new plate is being created at its western boundary ( $2 \text{ cm yr}^{-1}$ ); so eventually plate B will cease to exist on the surface of the planet.

If we introduce a third plate into the model, the motions become more complex still (Fig. 2.6(a)). In this example, plates A and B are spreading away from the ridge at a half-rate of  $2 \text{ cm yr}^{-1}$ , just as in Fig. 2.5(a). The eastern boundary of plates A and B is a subduction zone, with plate A being subducted beneath plate





**Figure 2.7.** (a) A three-plate model on a flat planet. Plate A is unshaded. The western boundary of plate B is a ridge from which seafloor spreads at a half-rate of  $2 \text{ cm yr}^{-1}$ . The boundary between plates A and C is a transform fault with relative motion of  $3 \text{ cm yr}^{-1}$ . (b) Relative velocity vectors for the plates shown in (a). (c) The stable solution to the model in (a): the northern boundary of plate B is a transform fault with a  $4 \text{ cm yr}^{-1}$  slip rate, and the boundary between plates B and C is a subduction zone with an oblique subduction rate of  $5 \text{ cm yr}^{-1}$ . (d) Vector addition to determine the velocity of plate B with respect to plate C,  ${}^C\mathbf{v}_B$ .

C at  $6 \text{ cm yr}^{-1}$ . The presence of plate C does not alter the relative motions across the northern and southern boundaries of plate B; these boundaries are transform faults just as in Fig. 2.5. To determine the relative rate of plate motion at the boundary between plates B and C, we must use vector addition:

$${}^C\mathbf{v}_B = {}^C\mathbf{v}_A + {}^A\mathbf{v}_B \quad (2.2)$$

This is demonstrated in Fig. 2.6(d): plate B is being subducted beneath plate C at  $10 \text{ cm yr}^{-1}$ . This means that the net rate of destruction of plate B is  $10 - 2 = 8 \text{ cm yr}^{-1}$ ; eventually, plate B will be totally subducted, and a simple two-plate subduction model will be in operation. However, if plate B were overriding plate C, it would be increasing in width by  $2 \text{ cm yr}^{-1}$ .

So far the examples have been straightforward in that all relative motions have been in an east–west direction. (Vector addition was not really necessary; common sense works equally well.) Now let us include motion in the north–south direction also. Figure 2.7(a) shows the model of three plates A, B and C: the western boundary of plate B is a ridge that is spreading at a half-rate of  $2 \text{ cm yr}^{-1}$ , the northern boundary of plate B is a transform fault (just as in the other examples)

and the boundary between plates A and C is a transform fault with relative motion of  $3 \text{ cm yr}^{-1}$ . The motion at the boundary between plates B and C is unknown and must be determined by using Eq. (2.2). For this example it is necessary to draw a vector triangle to determine  ${}_C\mathbf{v}_B$  (Fig. 2.7(d)). A solution to the problem is shown in Fig. 2.7(c): plate B undergoes oblique subduction beneath plate C at  $5 \text{ cm yr}^{-1}$ . The other possible solution is for plate C to be subducted beneath plate B at  $5 \text{ cm yr}^{-1}$ . In that case, the boundary between plates C and B would not remain collinear with the boundary between plates B and C but would move steadily to the east. (This is an example of the instability of a *triple junction*; see Section 2.6.)

These examples should give some idea of what can happen when plates move relative to each other and of the types of plate boundaries that occur in various situations. Some of the problems at the end of this chapter refer to a flat Earth, such as we have assumed for these examples. The real Earth, however, is spherical, so we need to use some spherical geometry.

### 2.3 Rotation vectors and rotation poles

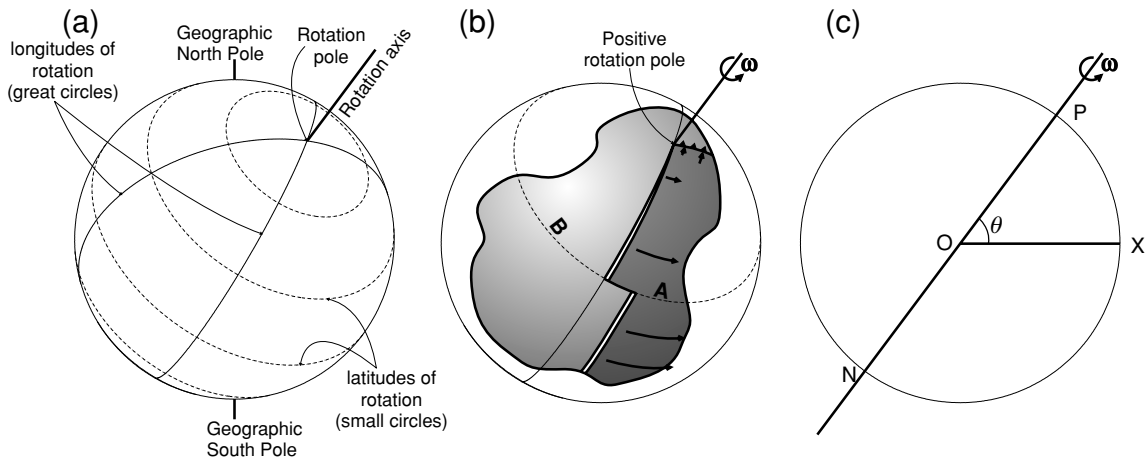
To describe motions on the surface of a sphere we use Euler's '*fixed-point*' theorem, which states that 'The most general displacement of a rigid body with a fixed point is equivalent to a rotation about an axis through that fixed point.'

Taking a plate as a rigid body and the centre of the Earth as a fixed point, we can restate this theorem: 'Every displacement from one position to another on the surface of the Earth can be regarded as a rotation about a suitably chosen axis passing through the centre of the Earth.'

This restated theorem was first applied by Bullard *et al.* (1965) in their paper on continental drift, in which they describe the fitting of the coastlines of South America and Africa. The 'suitably chosen axis' which passes through the centre of the Earth is called the *rotation axis*, and it cuts the surface of the Earth at two points called the *poles of rotation* (Fig. 2.8(a)). These are purely mathematical points and have no physical reality, but their positions describe the directions of motion of all points along the plate boundary. The magnitude of the angular velocity about the axis then defines the magnitude of the relative motion between the two plates. Because angular velocities behave as vectors, the relative motion between two plates can be written as  $\boldsymbol{\omega}$ , a vector directed along the rotation axis. The magnitude of  $\boldsymbol{\omega}$  is  $\omega$ , the angular velocity. The sign convention used is that a rotation that is clockwise (or right-handed) when viewed from the centre of the Earth along the rotation axis is positive. Viewed from outside the Earth, a positive rotation is anticlockwise. Thus, one rotation pole is positive and the other is negative (Fig. 2.8(b)).

Consider a point X on the surface of the Earth (Fig. 2.8(c)). At X the value of the relative velocity  $v$  between the two plates is

$$v = \omega R \sin \theta \quad (2.3)$$



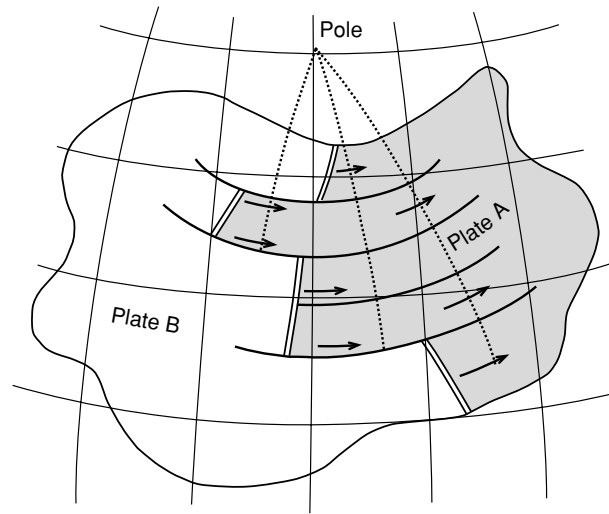
**Figure 2.8.** The movement of plates on the surface of the Earth. (a) The lines of latitude of rotation around the rotation poles are small circles (shown dashed) whereas the lines of longitude of rotation are great circles (i.e., circles with the same diameter as the Earth). Note that these lines of latitude and longitude are *not* the geographic lines of latitude and longitude because the poles for the geographic coordinate system are the North and South Poles, not the rotation poles. (b) Constructive, destructive and conservative boundaries between plates A and B. Plate B is assumed to be fixed so that the motion of plate A is relative to plate B. The visible rotation pole is positive (motion is anticlockwise when viewed from outside the Earth). Note that the spreading and subduction rates increase with distance from the rotation pole. The transform fault is an arc of a small circle (shown dashed) and thus is perpendicular to the ridge axis. As the plate boundary passes the rotation pole, the boundary changes from constructive to destructive, i.e. from ridge to subduction zone. (c) A cross section through the centre of the Earth O. P and N are the positive and negative rotation poles, and X is a point on the plate boundary.

where  $\theta$  is the angular distance between the rotation pole P and the point X, and  $R$  is the radius of the Earth. This factor of  $\sin \theta$  means that the relative motion between two adjacent plates changes with position along the plate boundary, in contrast to the earlier examples for a flat Earth. Thus, the relative velocity is zero at the rotation poles, where  $\theta = 0^\circ$  and  $180^\circ$ , and has a maximum value of  $\omega R$  at  $90^\circ$  from the rotation poles. If by chance the plate boundary passes through the rotation pole, the nature of the boundary changes from divergent to convergent, or vice versa (as in Fig. 2.8(b)). Lines of constant velocity (defined by  $\theta = \text{constant}$ ) are small circles about the rotation poles.

## 2.4 Present-day plate motions

### 2.4.1 Determination of rotation poles and rotation vectors

Several methods can be used to find the present-day *instantaneous poles of rotation* and *relative angular velocities* between pairs of plates. *Instantaneous* refers to a geological instant; it means a value averaged over a period of time ranging



**Figure 2.9.** On a spherical Earth the motion of plate A relative to plate B must be a rotation about some pole. All the transform faults on the boundary between plates A and B must be small circles about that pole. Transform faults can be used to locate the pole: it lies at the intersection of the great circles which are perpendicular to the transform faults. Although ridges are generally perpendicular to the direction of spreading, this is not a geometric requirement, so it is not possible to determine the relative motion or locate the pole from the ridge itself. (After Morgan (1968).)

from a few years to a few million years, depending on the method used. These methods include the following.

1. A local determination of the direction of relative motion between two plates can be made from the strike of active transform faults. Methods of recognizing transform faults are discussed fully in Section 8.5. Since transform faults on ridges are much easier to recognize and more common than transform faults along destructive boundaries, this method is used primarily to find rotation poles for plates on either side of a mid-ocean ridge. The relative motion at transform faults is parallel to the fault and is of constant value along the fault. This means that the faults are arcs of small circles about the rotation pole. The rotation pole must therefore lie somewhere on the great circle which is perpendicular to that small circle. So, if two or more transform faults can be used, the intersection of the great circles is the position of the rotation pole (Fig. 2.9).
2. The spreading rate along a constructive plate boundary changes as the sine of the angular distance  $\theta$  from the rotation pole (Eq. (2.3)). So, if the spreading rate at various locations along the ridge can be determined (from spacing of oceanic magnetic anomalies as discussed in Chapter 3), the rotation pole and angular velocity can then be estimated.
3. The analysis of data from an earthquake can give the direction of motion and the plane of the fault on which the earthquake occurred. This is known as a *fault-plane*

*solution* or a *focal mechanism* (discussed fully in Section 4.2.8). Fault-plane solutions for earthquakes along a plate boundary can give the direction of relative motion between the two plates. For example, earthquakes occurring on the transform fault between plates A and B in Fig. 2.8(b) would indicate that there is right lateral motion across the fault. The location of the pole and the direction, though not the magnitude, of the motion can thus be estimated.

4. Where plate boundaries cross land, surveys of displacements can be used (over large distances and long periods of time) to determine the local relative motion. For example, stream channels and even roads, field boundaries and buildings may be displaced.
5. Satellites have made it possible to measure instantaneous plate motions with some accuracy. One method uses a satellite laser-ranging system (SLR) to determine differences in distance between two sites on the Earth's surface over a period of years. Another method, very-long-baseline interferometry (VLBI), uses quasars for the signal source and terrestrial radio telescopes as the receivers. Again, the difference in distance between two telescope sites is measured over a period of years. Worldwide, the rates of plate motion determined by VLBI and SLR agree with geologically determined rates to within 2%.

A third method of measuring plate motions utilizes the Global Positioning System (GPS) which was developed to provide real-time navigation and positioning using satellites. A worldwide network of GPS receivers with a precision suitable for geodynamics has been established (1 cm in positioning and  $<10^{-3}$  arcsec in pole-position estimates). It is called the International GPS Service for Geodynamics (IGS), and is a permanent global network of receivers. Analysis of data from 1991–1996 shows that the agreement of GPS velocities with the geologically determined velocities for all but a few locations is to better than 95% confidence. This is another impressive corroboration of relative plate motions – *the plates are continually in motion*.

An estimate of the present-day plate motions, NUVEL-1A, made by using 277 measurements of ridge spreading rate, 121 oceanic transform-fault azimuths and 724 earthquake slip vectors is given in Table 2.1. Figure 2.10 shows velocities in southern California relative to North America as determined from geodetic measurements (including GPS and VLBI) between 1972 and 1995. The measured velocity of motion across this boundary was  $50 \text{ mm yr}^{-1}$ , compared with the  $49 \text{ mm yr}^{-1}$  predicted (Table 2.1). Thus again geological estimates based on measurements with a timescale of a million years agree with measurements made over a few years.

Although clear boundaries between rigid plates describe the relative motions and structures well, there are a few boundaries for which the term '*diffuse plate boundary*' is appropriate. The main examples are the North American and South American plate boundary from the Mid-Atlantic Ridge to the Caribbean and the boundary which subdivides the Indian plate.

It is important to realize that a rotation with a large angular velocity  $\omega$  does not necessarily mean that the relative motion along the plate boundary is also large.

Table 2.1 *Rotation vectors for the present-day relative motion between some pairs of plates: NUVEL-1A*

Plates	Positive-pole position		Angular velocity ( $10^{-7}$ deg yr $^{-1}$ )
	Latitude	Longitude	
Africa–Antarctica	5.6°N	39.2°W	1.3
Africa–Eurasia	21.0°N	20.6°W	1.2
Africa–North America	78.8°N	38.3°E	2.4
Africa–South America	62.5°N	39.4°W	3.1
Australia–Antarctica	13.2°N	38.2°E	6.5
Pacific–Antarctica	64.3°S	96.0°E	8.7
South America–Antarctica	86.4°S	139.3°E	2.6
Arabia–Eurasia	24.6°N	13.7°E	5.0
India–Eurasia	24.4°N	17.7°E	5.1
Eurasia–North America	62.4°N	135.8°E	2.1
Eurasia–Pacific	61.1°N	85.8°W	8.6
Pacific–Australia	60.1°S	178.3°W	10.7
North America–Pacific	48.7°N	78.2°W	7.5
Cocos–North America	27.9°N	120.7°W	13.6
Nazca–Pacific	55.6°N	90.1°W	13.6
Nazca–South America	56.0°N	94.0°W	7.2

*Note:* The first plate moves anticlockwise with respect to the second plate as shown.

*Source:* After DeMets *et al.* (1990; 1994).

**Figure 2.10.** Motion of southern California with respect to North America. Error ellipses represent 95% confidence. (After Shen *et al.* (1997). Crustal deformation measured in Southern California, *EOS Trans. Am. Geophys. Un.*, **78** (43), 477 and 482, 1997. Copyright 1997 American Geophysical Union. Reprinted by permission of American Geophysical Union)

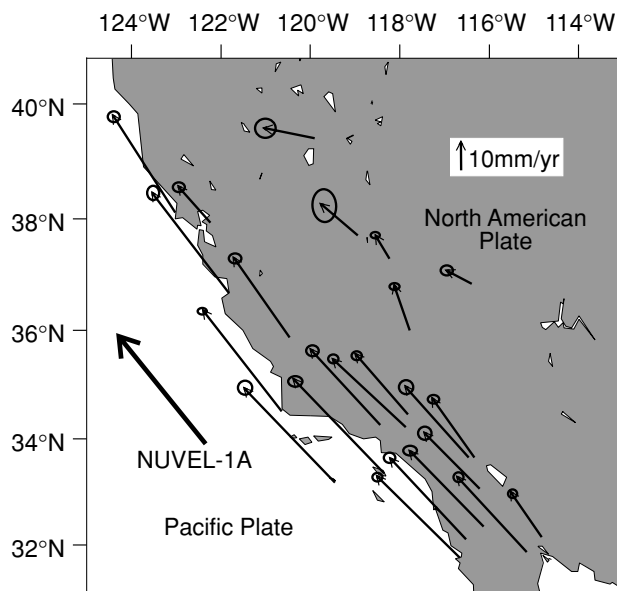
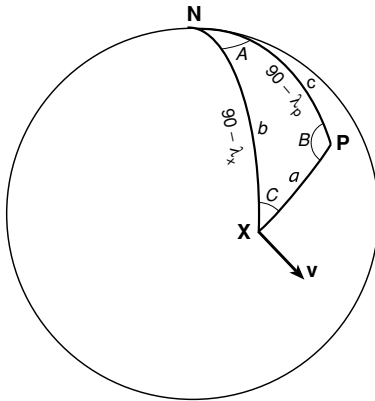


Table 2.2 *Symbols used in calculations involving rotation poles*

Symbol	Meaning	Sign convention
$\lambda_p$	Latitude of rotation pole P	$^{\circ}\text{N}$ positive
$\lambda_x$	Latitude of point X on plate boundary	$^{\circ}\text{S}$ negative
$\phi_p$	Longitude of rotation pole P	$^{\circ}\text{W}$ negative
$\phi_x$	Longitude of point X on plate boundary	$^{\circ}\text{E}$ positive
$\mathbf{v}$	Velocity of point X on plate boundary	
$v$	Amplitude of velocity $\mathbf{v}$	
$\beta$	Azimuth of the velocity with respect to north N	Clockwise positive
$R$	Radius of the Earth	
$\omega$	Angular velocity about rotation pole P	



**Figure 2.11.** A diagram showing the relative positions of the positive rotation pole P and point X on the plate boundary. N is the North Pole. The sides of the spherical triangle NPX are all great circles, the sides NX and NP are lines of geographic longitude. The vector  $\mathbf{v}$  is the relative velocity at point X on the plate boundary (note that  $\mathbf{v}$  is perpendicular to PX). It is usual to quote the lengths of the sides of spherical triangles as angles (e.g., latitude and longitude when used as geographic coordinates).

The distance between rotation pole and plate boundary is important (remember the  $\sin \theta$  factor multiplying the angular velocity  $\omega$  in Eq. (2.3)). However, it is conventional to use the relative velocity at  $\theta = 90^\circ$  when quoting a relative velocity for two plates, even though neither plate may extend  $90^\circ$  from the pole.

### 2.4.2 Calculation of the relative motion at a plate boundary

Once the instantaneous rotation pole and angular velocity for a pair of adjacent plates have been determined, they can be used to calculate the direction and magnitude of the relative motion at any point along the plate boundary.

The notation and sign conventions used in the following pages are given in Table 2.2. Figure 2.11 shows the relative positions of the North Pole N, positive rotation pole P and point X on the plate boundary (compare with Fig. 2.8(b)). In the spherical triangle NPX, let the angles  $\widehat{XNP} = A$ ,  $\widehat{NPX} = B$  and  $\widehat{PXN} = C$ ,

and let the angular lengths of the sides of the triangle be  $PX = a$ ,  $XN = b$  and  $NP = c$ . Thus, the angular lengths  $b$  and  $c$  are known, but  $a$  is not:

$$b = 90 - \lambda_x \quad (2.4)$$

$$c = 90 - \lambda_p \quad (2.5)$$

Angle  $A$  is known, but  $B$  and  $C$  are not:

$$A = \phi_p - \phi_x \quad (2.6)$$

Equation (2.3) is used to obtain the magnitude of the velocity at point X:

$$v = \omega R \sin a \quad (2.7)$$

The azimuth of the velocity,  $\beta$  is given by

$$\beta = 90 + C \quad (2.8)$$

To find the angles  $a$  and  $C$  needed for Eqs. (2.7) and (2.8), we use spherical geometry. Just as there are cosine and sine rules relating the angles and sides of plane triangles, there are cosine and sine rules for spherical triangles:

$$\cos a = \cos b \cos c + \sin b \sin c \cos A \quad (2.9)$$

and

$$\frac{\sin a}{\sin A} = \frac{\sin c}{\sin C} \quad (2.10)$$

Substituting Eqs. (2.4)–(2.6) into Eq. (2.9) gives

$$\begin{aligned} \cos a &= \cos(90 - \lambda_x) \cos(90 - \lambda_p) \\ &+ \sin(90 - \lambda_x) \sin(90 - \lambda_p) \cos(\phi_p - \phi_x) \end{aligned} \quad (2.11)$$

This can then be simplified to yield the angle  $a$ , which is needed to calculate the velocity from Eq. (2.7):

$$a = \cos^{-1}[\sin \lambda_x \sin \lambda_p + \cos \lambda_x \cos \lambda_p \cos(\phi_p - \phi_x)] \quad (2.12)$$

Substituting Eqs. (2.5) and (2.6) into Eq. (2.10) gives

$$\frac{\sin a}{\sin(\phi_p - \phi_x)} = \frac{\sin(90 - \lambda_p)}{\sin C} \quad (2.13)$$

Upon rearrangement this becomes

$$C = \sin^{-1} \left( \frac{\cos \lambda_p \sin(\phi_p - \phi_x)}{\sin a} \right) \quad (2.14)$$

Therefore, if the angle  $a$  is calculated from Eq. (2.12), angle  $C$  can then be calculated from Eq. (2.14), and, finally, the relative velocity and its azimuth can be calculated from Eqs. (2.7) and (2.8). Note that the inverse sine function of Eq. (2.14) is double-valued.<sup>1</sup> Always check that you have the correct value for  $C$ .

<sup>1</sup> An alternative way to calculate motion along a plate boundary and to avoid the sign ambiguities is to use vector algebra (see Altman (1986) or Cox and Hart (1986), p. 154).



**Example: calculation of relative motion at a plate boundary**

Calculate the present-day relative motion at 28°S, 71°W on the Peru–Chile Trench using the Nazca–South America rotation pole given in Table 2.1. Assume the radius of the Earth to be 6371 km:

$$\lambda_x = -28^\circ, \quad \phi_x = -71^\circ$$

$$\lambda_p = 56^\circ, \quad \phi_p = -94^\circ$$

$$\omega = 7.2 \times 10^{-7} \text{ deg yr}^{-1} = \frac{\pi}{180} \times 7.2 \times 10^{-7} \text{ rad yr}^{-1}$$

These values are substituted into Eqs. (2.12), (2.14), (2.7) and (2.8) in that order, giving

$$\begin{aligned} a &= \cos^{-1}[\sin(-28)\sin(56) + \cos(-28)\cos(56)\cos(-94 + 71)] \\ &= 86.26^\circ \end{aligned} \quad (2.15)$$

$$\begin{aligned} C &= \sin^{-1}\left(\frac{\cos(56)\sin(-94 + 71)}{\sin(86.26)}\right) \\ &= -12.65^\circ \end{aligned} \quad (2.16)$$

$$\begin{aligned} v &= \frac{\pi}{180} \times 7.2 \times 10^{-7} \times 6371 \times 10^5 \times \sin(86.26) \\ &= 7.97 \text{ cm yr}^{-1} \end{aligned} \quad (2.17)$$

$$\begin{aligned} \beta &= 90 - 12.65 \\ &= 77.35^\circ \end{aligned} \quad (2.18)$$

Thus, the Nazca plate is moving relative to the South American plate at 8 cm yr<sup>-1</sup> with azimuth 77°; the South American plate is moving relative to the Nazca plate at 8 cm yr<sup>-1</sup>, azimuth 257° (Fig. 2.2).

**2.4.3 Combination of rotation vectors**

Suppose that there are three rigid plates A, B and C and that the angular velocity of A relative to B,  ${}_B\omega_A$ , and that of B relative to C,  ${}_C\omega_B$ , are known. The motion of plate A relative to plate C,  ${}_C\omega_A$ , can be determined by vector addition just as for the flat Earth:

$${}_C\omega_A = {}_C\omega_B + {}_B\omega_A \quad (2.19)$$

(Remember that in this notation the first subscript refers to the ‘fixed’ plate.) Alternatively, since  ${}_B\omega_A = -{}_A\omega_B$ , Eq. (2.19) can be written as

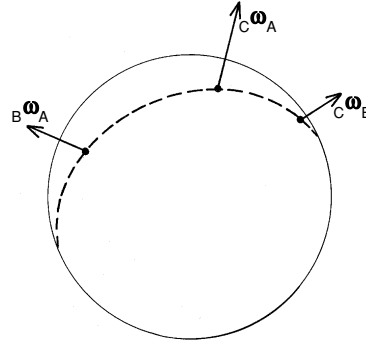
$${}_A\omega_B + {}_B\omega_C + {}_C\omega_A = 0 \quad (2.20)$$

The resultant vector  ${}_C\omega_A$  of Eq. (2.19) must lie in the same plane as the two original vectors  ${}_B\omega_A$  and  ${}_C\omega_B$ . Imagine the great circle on which these two poles

Table 2.3 *Notation used in addition of rotation vectors*

Rotation vector	Magnitude	Latitude of pole	Longitude of pole
${}_B\omega_A$	${}_B\omega_A$	$\lambda_{BA}$	$\phi_{BA}$
${}_C\omega_B$	${}_C\omega_B$	$\lambda_{CB}$	$\phi_{CB}$
${}_C\omega_A$	${}_C\omega_A$	$\lambda_{CA}$	$\phi_{CA}$

**Figure 2.12.** Relative-rotation vectors  ${}_B\omega_A$  and  ${}_C\omega_A$  for the plates A, B and C. The dashed line is the great circle on which the two poles lie. The resultant rotation vector is  ${}_C\omega_A$  (Eq. (2.19)). The resultant pole must also lie on the same great circle because the resultant rotation vector has to lie in the plane of the two original rotation vectors.



lie; the resultant pole must also lie on that same great circle (Fig. 2.12). Note that this relationship (Eqs. (2.19) and (2.20)) should be used only for infinitesimal movements or angular velocities, not for finite rotations. The theory of finite rotations is complex. (For a treatment of the whole theory of instantaneous and finite rotations, the reader is referred to Le Pichon *et al.* (1973).)

Let the three vectors  ${}_B\omega_A$ ,  ${}_C\omega_B$  and  ${}_C\omega_A$  be written as shown in Table 2.3. It is simplest to use a rectangular coordinate system through the centre of the Earth, with the  $x$ - $y$  plane being equatorial, the  $x$  axis passing through the Greenwich meridian and the  $z$  axis passing through the North Pole, as shown in Fig. 2.13. The sign convention of Table 2.2 continues to apply. Then Eq. (2.19) can be written

$$x_{CA} = x_{CB} + x_{BA} \quad (2.21)$$

$$y_{CA} = y_{CB} + y_{BA} \quad (2.22)$$

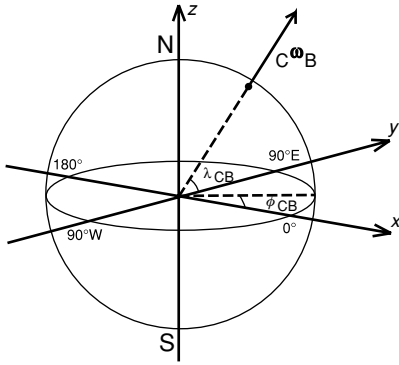
$$z_{CA} = z_{CB} + z_{BA} \quad (2.23)$$

where  $x_{BA}$ ,  $y_{BA}$  and  $z_{BA}$  are the  $x$ ,  $y$  and  $z$  coordinates of the vector  ${}_B\omega_A$ , and so on. Equations (2.21)–(2.23) become

$$x_{CA} = {}_C\omega_B \cos \lambda_{CB} \cos \phi_{CB} + {}_B\omega_A \cos \lambda_{BA} \cos \phi_{BA} \quad (2.24)$$

$$y_{CA} = {}_C\omega_B \cos \lambda_{CB} \sin \phi_{CB} + {}_B\omega_A \cos \lambda_{BA} \sin \phi_{BA} \quad (2.25)$$

$$z_{CA} = {}_C\omega_B \sin \lambda_{CB} + {}_B\omega_A \sin \lambda_{BA} \quad (2.26)$$



**Figure 2.13.** The rectangular coordinate system used in the addition of rotation vectors. The  $x$ - $y$  plane is equatorial with the  $x$  axis passing through  $0^\circ$  Greenwich and the  $z$  axis through the North Pole. Notation and sign conventions are given in Table 2.3.

when the three rotation vectors are expressed in their  $x$ ,  $y$  and  $z$  components. The magnitude of the resultant rotation vector,  $C\omega_A$ , is

$$C\omega_A = \sqrt{x_{CA}^2 + y_{CA}^2 + z_{CA}^2} \quad (2.27)$$

and the pole position is given by

$$\lambda_{CA} = \sin^{-1} \left( \frac{z_{CA}}{C\omega_A} \right) \quad (2.28)$$

and

$$\phi_{CA} = \tan^{-1} \left( \frac{y_{CA}}{x_{CA}} \right) \quad (2.29)$$

Note that this expression for  $\phi_{CA}$  has an ambiguity of  $180^\circ$  (e.g.,  $\tan 30^\circ = \tan 210^\circ = 0.5774$ ,  $\tan 110^\circ = \tan 290^\circ = -2.747$ ). This is resolved by adding or subtracting  $180^\circ$  so that

$$x_{CA} > 0 \quad \text{when } -90^\circ < \phi_{CA} < +90^\circ \quad (2.30)$$

$$x_{CA} < 0 \quad \text{when } |\phi_{CA}| > 90^\circ \quad (2.31)$$

The problems at the end of this chapter enable the reader to use these methods to determine motions along real and imagined plate boundaries.

#### Example: addition of relative rotation vectors

Given the instantaneous rotation vectors in Table 2.1 for the Nazca plate relative to the Pacific plate and the Pacific plate relative to the Antarctic plate, calculate the instantaneous rotation vector for the Nazca plate relative to the Antarctic plate.

Plate	Rotation vector	Latitude of pole	Longitude of pole	Angular velocity ( $10^{-7} \text{ deg yr}^{-1}$ )
Nazca–Pacific	$P\omega_N$	$55.6^\circ \text{N}$	$90.1^\circ \text{W}$	13.6
Pacific–Antarctica	$A\omega_P$	$64.3^\circ \text{S}$	$96.0^\circ \text{E}$	8.7

To calculate the rotation vector for the Nazca plate relative to the Antarctic plate we apply Eq. (2.19):

$${}_A\omega_N = {}_A\omega_P + {}_P\omega_N \quad (2.32)$$

Substituting the tabulated values into the equations for the  $x$ ,  $y$  and  $z$  components of  ${}_A\omega_N$  (Eqs. (2.24)–(2.26)) yields

$$\begin{aligned} x_{AN} &= 8.7 \cos(-64.3) \cos(96.0) + 13.6 \cos(55.6) \cos(-90.1) \\ &= -0.408 \end{aligned} \quad (2.33)$$

$$\begin{aligned} y_{AN} &= 8.7 \cos(-64.3) \sin(96.0) + 13.6 \cos(55.6) \sin(-90.1) \\ &= -3.931 \end{aligned} \quad (2.34)$$

$$\begin{aligned} z_{AN} &= 8.7 \sin(-64.3) + 13.6 \sin(55.6) \\ &= 3.382 \end{aligned} \quad (2.35)$$

The magnitude of the rotation vector  ${}_A\omega_N$  can now be calculated from Eq. (2.27) and the pole position from Eqs. (2.28) and (2.29):

$${}_A\omega_N = \sqrt{0.408^2 + 3.931^2 + 3.382^2} = 5.202 \quad (2.36)$$

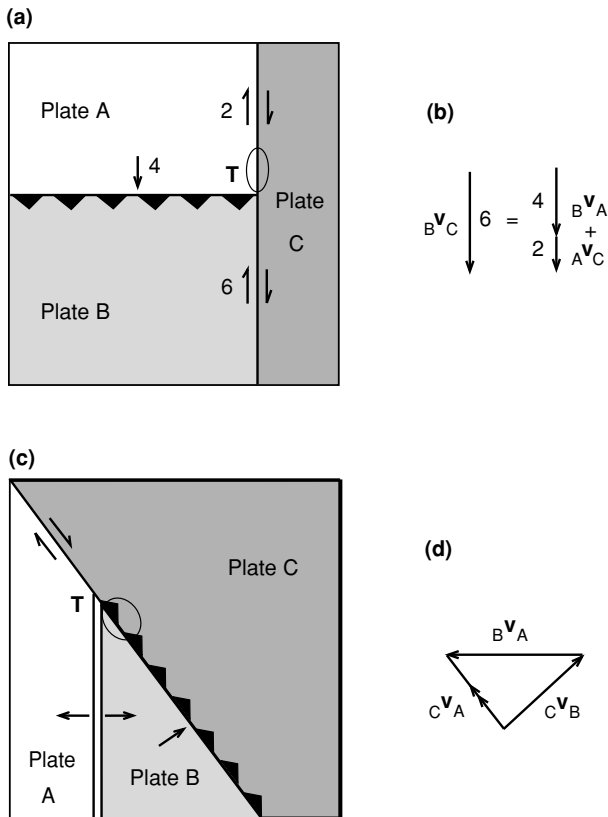
$$\lambda_{AN} = \sin^{-1} \left( \frac{3.382}{5.202} \right) = 40.6 \quad (2.37)$$

$$\phi_{AN} = \tan^{-1} \left( \frac{-3.931}{-0.408} \right) = 180 + 84.1 \quad (2.38)$$

Therefore, the rotation for the Nazca plate relative to the Antarctic plate has a magnitude of  $5.2 \times 10^{-7} \text{ deg yr}^{-1}$ , and the rotation pole is located at latitude  $40.6^\circ\text{N}$ , longitude  $95.9^\circ\text{W}$ .

## 2.5 Plate boundaries can change with time

The examples of plates moving upon a flat Earth (Section 2.2) illustrated that plates and plate boundaries do not stay the same for all time. This observation remains true when we advance from plates moving on a flat model Earth to plates moving on a spherical Earth. The formation of new plates and destruction of existing plates are the most obvious global reasons why plate boundaries and relative motions change. For example, a plate may be lost down a subduction zone, such as happened when most of the Farallon and Kula plates were subducted under the North American plate in the early Tertiary (see Section 3.3.3). Alternatively, two continental plates may coalesce into one (with resultant mountain building). If the position of a rotation pole changes, all the relative motions also change. A drastic change in pole position of say  $90^\circ$  would, of course, completely alter the status quo: transform faults would become ridges and subduction zones, and vice versa! Changes in the trends of transform faults and magnetic anomalies on the Pacific plate imply that the direction of seafloor spreading has changed there,



and indicate that the Pacific–Farallon pole position changed slightly a number of times during the Tertiary.

Parts of plate boundaries can change locally, however, without any major ‘plate’ or ‘pole’ event occurring. Consider three plates A, B and C. Let there be a convergent boundary between plates A and B, and let there be strike–slip faults between plates A and C and plates B and C, as illustrated in Figs. 2.14(a) and (b). From the point of view of an observer on plate C, part of the boundary of C (circled) will change with time because the plate to which it is adjacent will change from plate A to plate B. The boundary will remain a dextral (right-handed) fault, but the slip rate will change from 2 cm yr<sup>-1</sup> to 6 cm yr<sup>-1</sup>. Relative to plate C, the subduction zone is moving northwards at 6 cm yr<sup>-1</sup>. Another example of this type of plate-boundary change is illustrated in Figs. 2.14(c) and (d). In this case, the relative velocities are such that the boundary between plates A and C is a strike–slip fault, that between plates A and B is a ridge and that between plates B and C is a subduction zone. The motions are such that the ridge migrates slowly to the south relative to plate C, so the circled portion of plate boundary will change with time from subduction zone to transform fault.

These local changes in the plate boundary are a geometric consequence of the motions of the three rigid plates rather than being caused by any disturbing outside event. A complete study of all possible interactions of three plates is made in the next section. Such a study is very important because it enables us to apply the theory of rigid geometric plates to the Earth and deduce past plate motions from evidence in the local geological record. We can also predict details of future plate interactions.

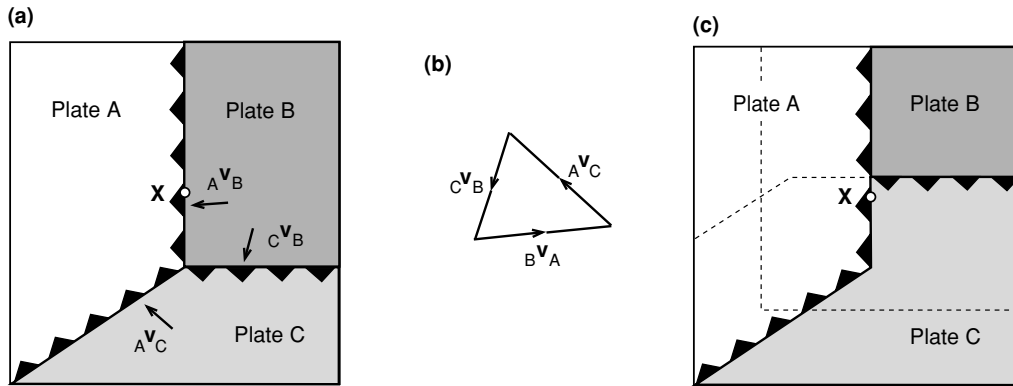
## 2.6 Triple junctions

### 2.6.1 Stable and unstable triple junctions

A *triple junction* is the name given to a point at which three plates meet, such as the points T in Fig. 2.14. A triple junction is said to be ‘stable’ when the relative motions of the three plates and the azimuth of their boundaries are such that the configuration of the junction does not change with time. The two examples shown in Fig. 2.14 are thus stable. In both cases the triple junction moves along the boundary of plate C, locally changing this boundary. The relative motions of the plates and triple junction and the azimuths and types of plate boundaries of the whole system do not change with time. An ‘unstable’ triple junction exists only momentarily before evolving to a different geometry. If four or more plates meet at one point, the configuration is always unstable, and the system will evolve into two or more triple junctions.

As a further example, consider a triple junction where three subduction zones meet (Fig. 2.15): plate A is overriding plates B and C, and plate C is overriding plate B. The relative-velocity triangle for the three plates at the triple junction is shown in Fig. 2.15(b). Now consider how this triple junction evolves with time. Assume that plate A is fixed; then the positions of the plates at some later time are as shown in Fig. 2.15(c). The dashed boundaries show the extent of the subducted parts of plates B and C. The subduction zone between plates B and C has moved north along the north–south edge of plate A. Thus, the original triple junction (Fig. 2.15(a)) was unstable; however, the new triple junction (Fig. 2.15(c)) is stable (meaning that its geometry and the relative velocities of the plates are unchanging), though the triple junction itself continues to move northwards along the north–south edge of plate A. The point X is originally on the boundary of plates A and B. As the triple junction passes X, an observer there will see a sudden change in subduction rate and direction. Finally, X is a point on the boundary of plates A and C.

In a real situation, the history of the northward passage of the triple junction along the boundary of plates A and C could be determined by estimating the time at which the relative motion between the plates changed at a number of locations along the boundary. If such time estimates increase regularly with position along the plate boundary, it is probable that a triple junction migrated along

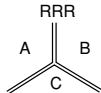
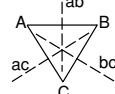
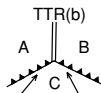
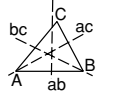
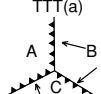
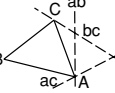
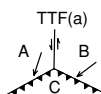

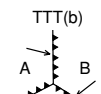
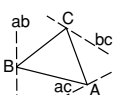
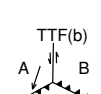
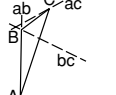
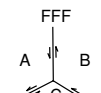
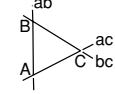
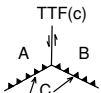
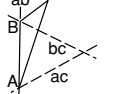
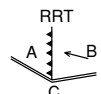
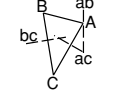
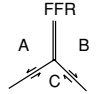
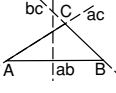
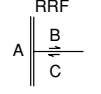
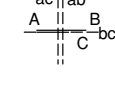
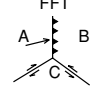
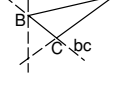
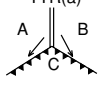
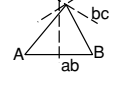
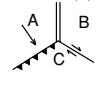
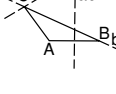
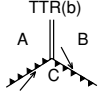
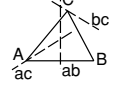
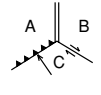
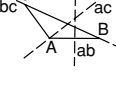


**Figure 2.15.** (a) A triple junction where three subduction zones intersect. Plate A overrides plates B and C, while plate C overrides plate B.  $A \mathbf{v}_B$ ,  $C \mathbf{v}_B$  and  $A \mathbf{v}_C$  are the relative velocities of the three plates in the immediate vicinity of the triple junction. (b) The relative-velocity triangle for (a). (c) The geometry of the three subduction zones at some time later than in (a). The dashed lines show where plates B and C would have been had they not been subducted. The point X in (a) was originally on the boundary between plates A and B; now it is on the boundary between plates A and C. The original triple junction has changed its form. (After McKenzie and Morgan (1969).)

the boundary. The alternative, a change in relative motion between the plates, would occur at one time. It can be seen that, although the original triple junction shown in Fig. 2.15(a) is not stable, it would be stable if  $A \mathbf{v}_C$  were parallel to the boundary between plates B and C. Then the boundary between B and C would not move in a north–south direction relative to A, so the geometry of the triple junction would be unchanging with time. The other configuration in which the triple junction would be stable occurs when the edge of the plate either side of the triple junction is straight. This is, of course, the final configuration illustrated in Fig. 2.15(c).

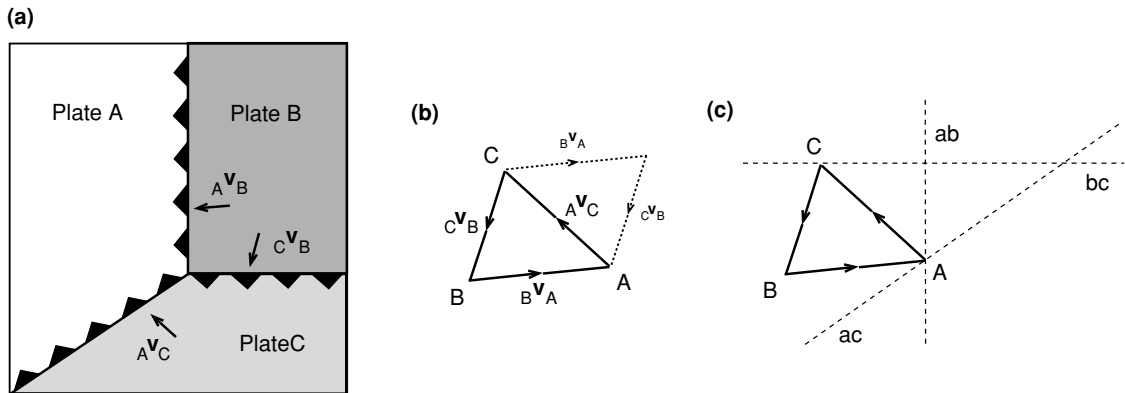
Altogether there are sixteen possible types of triple junction, all shown in Fig. 2.16. Of these sixteen triple junctions, one is always stable (the ridge–ridge–ridge junction) if oblique spreading is not allowed, and two are always unstable (the fault–fault–fault and fault–ridge–ridge junctions). The other thirteen junctions are stable under certain conditions. In the notation used to classify the types of triple junction, a ridge is written as R, a transform fault as F and a subduction zone (or trench) as T. Thus, a ridge–ridge–ridge junction is RRR, a fault–fault–ridge junction is FFR, and so on.

To examine the stability of any particular triple junction, it is easiest to draw the azimuths of the plate boundaries onto the relative velocity triangle. In Fig. 2.16 the lengths of the lines AB, BC and AC are proportional and parallel to the relative velocities  $A \mathbf{v}_B$ ,  $B \mathbf{v}_C$  and  $A \mathbf{v}_C$ . Thus, the triangles are merely velocity triangles such as that shown in Fig. 2.15(b). The triple junction of Fig. 2.15, type

Geometry	Velocity triangle	Stability	Possible Examples	Geometry	Velocity triangle	Stability	Possible Examples
		All orientations stable	East Pacific Rise and Galapagos Rift Zone, Indian Ocean Triple Junction			Stable if the angles between ab and ac, bc, respectively, are equal, or if ac, bc form a straight line	
		Stable if ab, ac form a straight line, or if bc is parallel to the slip vector CA	Central Japan			Stable if ac, bc form a straight line, or if C lies on ab	Intersection of the Peru-Chile trench and the Chile Rise
		Stable if the complicated general condition for ab, bc and ac to meeting at a point is satisfied				Stable if bc, ab form a straight line, or if ac goes through B	
		Unstable				Stable if ab, ac form a straight line, or if ab, bc do so	
		ab must go through centroid of ABC				Stable if C lies on ab, or if ac, bc form a straight line	Owen fracture zone and the Carlsberg Ridge, Chile Rise and the East Pacific Rise
		Unstable, evolves to FFR; but stable if ab and ac are perpendicular				Stable if ab, bc form a straight line, or if ac, bc do so	San Andreas Fault and Mendocino fracture zone (Mendocino triple junction)
		Stable if ab goes through C, or if ac, bc form a straight line				Stable if ab goes through C or if ac, bc form a straight line	Mouth of the Gulf of California (Rivera triple junction)
		Stable if complicated general conditions are satisfied				Stable if ac, ab cross on bc	

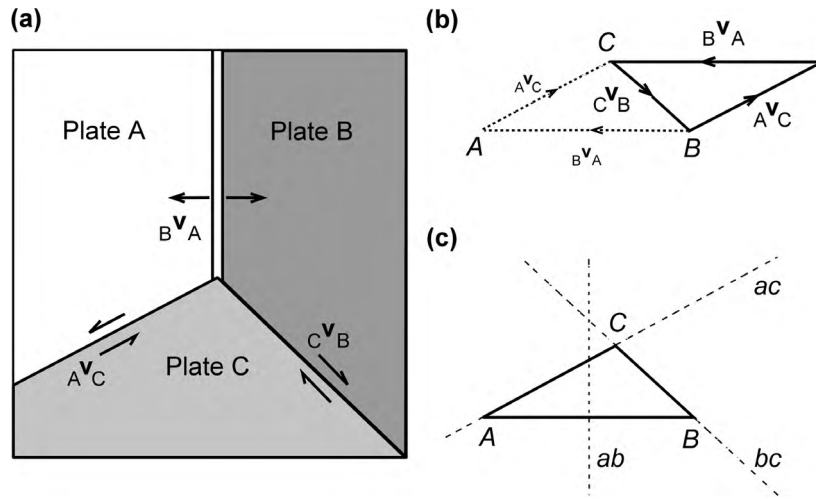
**Figure 2.16.** The geometry and stability of all possible triple junctions. In the categories represented by RRR, RTT, RTF and so on, R denotes ridge, T trench and F transform fault. The dashed lines ab, bc and ac in the velocity triangles represent velocities that leave the geometry of the boundary between plates A and B, B and C and A and C, respectively, unchanged. A triple junction is stable if ab, bc and ac meet at a point. Only an RRR triple junction (with ridges spreading symmetrically and perpendicular to their strikes) is always stable. (After McKenzie and Morgan (1969).)





**Figure 2.17.** Determination of stability for a triple junction involving three subduction zones, TTT(a) of Fig. 2.16. (a) The geometry of the triple junction and relative velocities; this is the same example as Fig. 2.15(a). (b) Relative-velocity triangles (Fig. 2.15(b)). Sides BA, CB and AC represent  $B \mathbf{v}_A$ ,  $C \mathbf{v}_B$  and  $A \mathbf{v}_C$ , respectively. The corner C represents the velocity of plate C. Thus for example, relative to plate A, the velocity of plate C,  $A \mathbf{v}_C$ , is represented by the line from point A to point C, and the line from point B to point A represents  $B \mathbf{v}_A$ , the velocity of plate A relative to plate B. (c) The dashed lines ab, ac, and bc drawn onto the velocity triangle ABC represent possible velocities of the boundary between plates A and B, plates A and C and plates B and C, respectively, which leave the geometry of those boundaries unchanged. The triple junction is stable if these three dashed lines intersect at a point. In this example, that would occur if ab were parallel to ac or if the velocity  $A \mathbf{v}_C$  were parallel to bc. If the geometry of the plate boundaries and the relative velocities at the triple junction do not satisfy either of these conditions, then the triple junction is unstable. If it is unstable, the geometry of the plate boundaries will change; this particular geometry and triple junction can exist only momentarily in geological time.

TTT(a) in Fig. 2.16, is shown in Fig. 2.17. The subduction zone between plates A and B does not move relative to plate A because plate A is overriding plate B. However, because all parts of the subduction zone look alike, any motion of the subduction zone parallel to itself would also satisfy this condition. Therefore, we can draw onto the velocity triangle a dashed line ab, which passes through point A and has the strike of the boundary between plates A and B (Fig. 2.17(c)). This line represents the possible velocities of the boundary between plates A and B which leave the geometry of these two plates unchanged. Similarly, we can draw a line bc that has the strike of the boundary between plates B and C and passes through point C (since the subduction zone is fixed on plate C) and a line ac that passes through point A and has the strike of the boundary between plates A and C. The point at which the three dashed lines ab, bc and ac meet represents the velocity of a stable triple junction. Clearly, in Fig. 2.17(c), these three lines do not meet at a point; therefore, this particular plate-boundary configuration is unstable. However, the three dashed lines would meet at a point (and the triple



**Figure 2.18.** Determination of stability for a triple junction involving a ridge and two transform faults, FFR, (a) The geometry of the triple junction and relative velocities. (b) Relative-velocity triangles (notation as for Fig. 2.17(b)). (c) Dashed lines drawn onto the relative-velocity triangle as for Fig. 2.17(c). This triple junction is stable if point C lies on the line  $ab$ , or if  $ac$  and  $bc$  are collinear. The first condition is satisfied if the triangle  $ABC$  is isosceles (i.e., the two transform faults are mirror images of each other). The second condition is satisfied if the boundary of plate C with plates A and B is straight.

junction would be stable) if  $bc$  were parallel to  $AC$  or if  $ab$  and  $ac$  were parallel. This would mean that either the relative velocity between plates A and C,  $A \mathbf{v}_C$ , was parallel to the boundary between plates B and C or the entire boundary of plate A was straight. These are the only two possible situations in which such a TTT triple junction is stable. By plotting the lines  $ab$ ,  $bc$  and  $ac$  onto the relative-velocity triangle, we can obtain the stability conditions more easily than we did in Fig. 2.15.

Figure 2.18 illustrates the procedure for a triple junction involving a ridge and two transform faults (type FFR). In this case,  $ab$ , the line representing any motion of the triple junction along the ridge, must be the perpendicular bisector of  $AB$ . In addition  $bc$  and  $ac$ , representing motion along the faults, are collinear with  $BC$  and  $AC$ . This type of triple junction is stable only if line  $ab$  goes through point C (both transform faults have the same slip rate) or if  $ac$  and  $bc$  are collinear (the boundary of plate C is straight). Choosing  $ab$  to be the perpendicular bisector of  $AB$  assumes that the ridge is spreading symmetrically and at right angles to its strike. This is usually the case. However, if the ridge does not spread symmetrically and/or at right angles to its strike, then  $ab$  must be drawn accordingly, and the stability conditions are different.

Figure 2.16 gives the conditions for stability of the various types of triple junction and also gives examples of some of the triple junctions occurring around the Earth at present. Many research papers discuss the stability or instability of the Mendocino and Queen Charlotte triple junctions that lie off western North America. These are the junctions (at the south and north ends, respectively) of the Juan de Fuca plate with the Pacific and North American plates and so are subjects of particular interest to North Americans because they involve the San Andreas Fault in California and the Queen Charlotte Fault in British Columbia. Another triple junction in that part of the Pacific is the Galapagos triple junction, where the Pacific, Cocos and Nazca plates meet; it is an RRR junction and thus is stable.

### 2.6.2 The significance of triple junctions

Work on the Mendocino triple junction, at which the Juan de Fuca, Pacific and North American plates meet at the northern end of the San Andreas Fault, shows why the stability of triple junctions is important for continental geology. The Mendocino triple junction is an FFT junction involving the San Andreas Fault, the Mendocino transform fault and the Cascade subduction zone. It is stable, as seen in Fig. 2.16, provided that the San Andreas Fault and the Cascade subduction zone are collinear. It has, however, been suggested that the Cascade subduction zone is after all not exactly collinear with the San Andreas Fault and, thus, that the Mendocino triple junction is unstable. This instability would result in the northwards migration of the triple junction and the internal deformation of the continental crust of the western U.S.A. along pre-existing zones of weakness. It would also explain many features such as the clockwise rotation of major blocks, such as the Sierra Nevada, and the regional extension and eastward stepping of the San Andreas transform. The details of the geometry of this triple junction are obviously of great importance to the regional evolution of the entire western U.S.A. Much of the geological history of the area over approximately the past thirty million years may be related to the migration of the triple junction, so a detailed knowledge of the plate motions is essential background for any explanation of the origin of Tertiary structures in this region. This subject is discussed further in Section 3.3.3. The motions of offshore plates can produce major structural changes even in the continents.

The Dead Sea Fault is similar to the San Andreas Fault system in that it is an intra-continental plate boundary. It is the boundary between the Arabian and African plates and extends northwards from the Red Sea to the East Anatolian Fault (Fig. 10.18). It is a left-lateral strike-slip fault with a slip rate of  $\sim 5 \text{ mm yr}^{-1}$ . That such a major strike-slip boundary is located close to the continental edge, but still within the continent, is because that is where the plate is weakest – a thinned continental margin is weaker than both oceanic and continental lithosphere. The

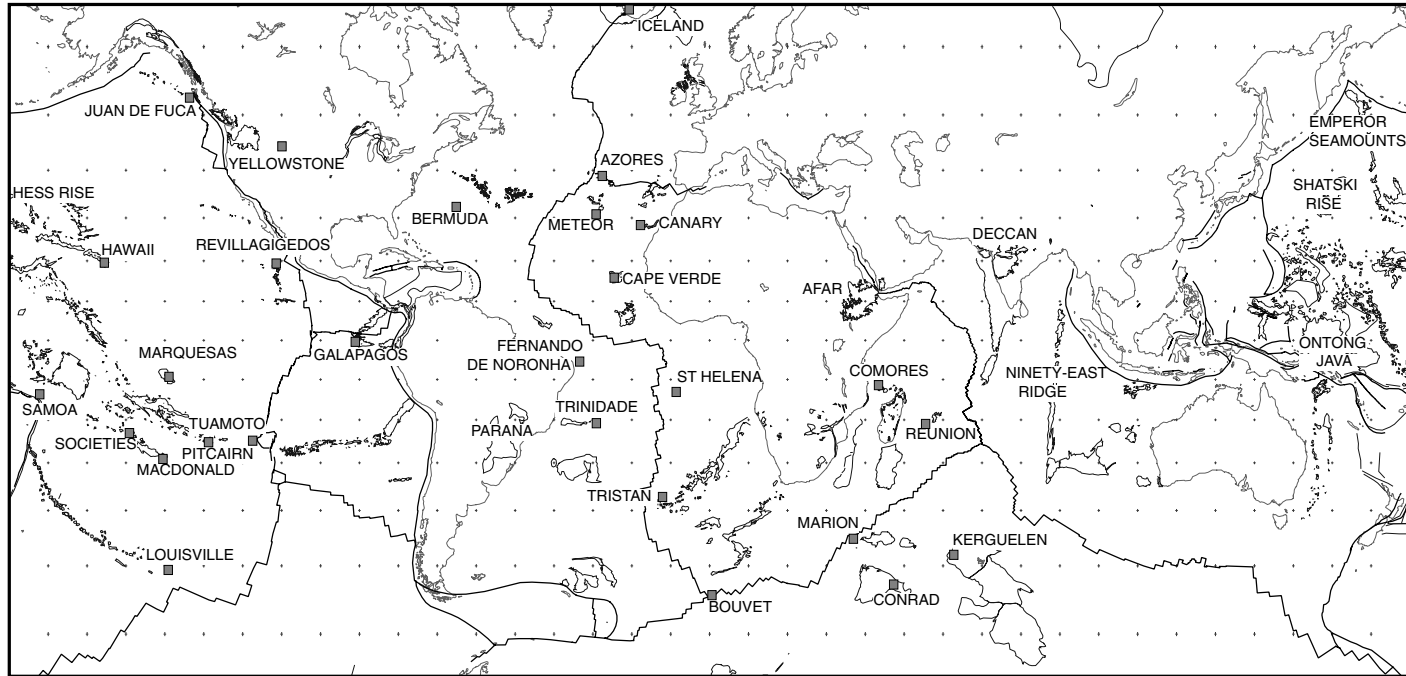
NUVEL-1A rotation pole for Africa–Arabia is at 24°N, but, in order for the motion along the boundary to be strike–slip, either the pole should be some 6° further north, or Sinai must be moving separately relative to Africa.

## 2.7 Absolute plate motions

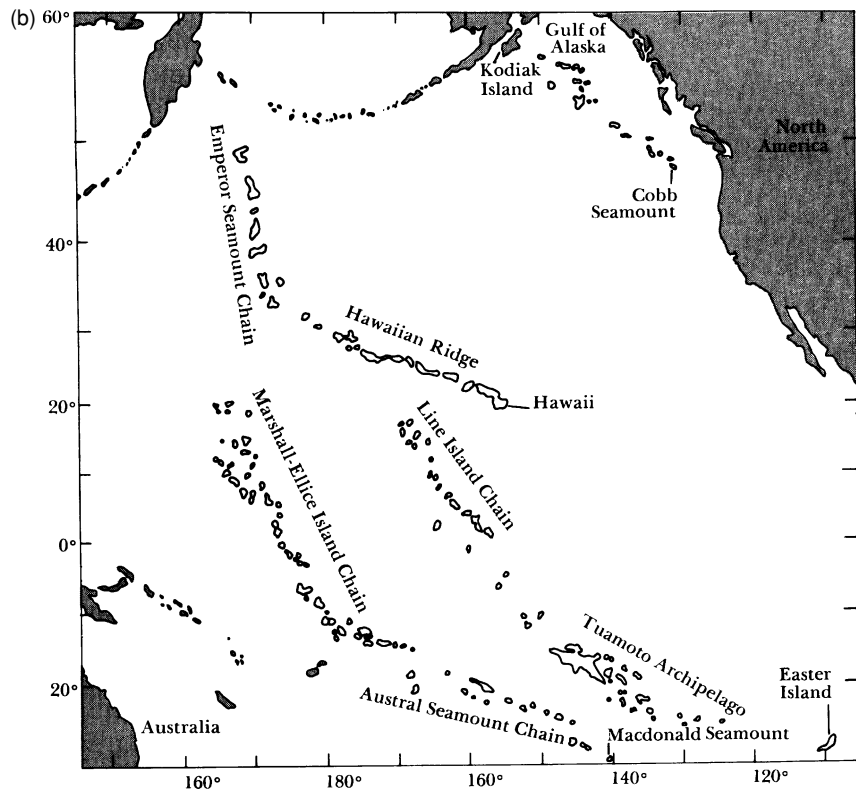
Although most of the volcanism on the Earth's surface is associated with the boundaries of plates, along the mid-ocean ridges and subduction zones, some isolated volcanic island chains occur in the oceans (Fig. 2.19(a)). These chains of oceanic islands are unusual in several respects: they occur well away from the plate boundaries (i.e., they are *intraplate volcanoes*); the chemistry of the erupted lavas is significantly different from that of both mid-ocean-ridge and subduction-zone lavas; the active volcano may be at one end of the island chain, with the islands ageing with distance from that active volcano; and the island chains appear to be arcs of small circles. These features, taken together, are consistent with the volcanic islands having formed as the plate moved over what is colloquially called a *hotspot*, a place where melt rises from deep in the mantle. Figure 2.19(b) shows four volcanic island and seamount chains in the Pacific Ocean. There is an active volcano at the southeastern end of each of the island chains. The Emperor–Hawaiian seamount chain is the best defined and most studied. The ages of the seamounts increase steadily from Loihi (the youngest and at present active) a submarine volcano off the southeast coast of the main island of Hawaii, north-westwards through the Hawaiian chain. There is a pronounced change in strike of the chain where the volcanic rocks are about forty-three million years (43 Ma) old. The northern end of the Emperor seamount chain near the Kamchatka peninsula of Russia is 78 Ma old. The change in strike at 43 Ma can most simply be explained by a change in the direction of movement of the Pacific plate over the hotspot at that time. The chemistry of oceanic-island lavas is discussed in Section 7.8.3 and the structure of the islands themselves in Section 9.7.

All the plate motions described so far in this chapter have been relative motions, that is, motions of the Pacific plate relative to the North American plate, the African plate relative to the Eurasian plate, and so on. There is no fixed point on the Earth's surface. Absolute plate motions are motions of the plates relative to some imaginary fixed point. One way of determining absolute motions is to suppose that the Earth's mantle moves much more slowly than the plates so that it can be regarded as nearly fixed. Such absolute motions can be calculated from the traces of the oceanic island chains or the traces of continental volcanism, which are assumed to have formed as the plate passed over a hotspot with its source fixed in the mantle. The absolute motion of a plate, the Pacific, for example, can be calculated from the traces of the oceanic island and seamount chains on it. The absolute motions of all the other plates can then be calculated from their motion relative to the Pacific plate. Repeating the procedure, using hotspot traces from other plates, gives some idea of the validity of the assumption that hotspots are fixed.

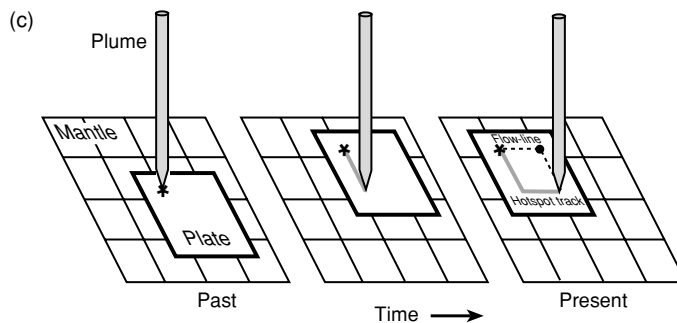
(a)



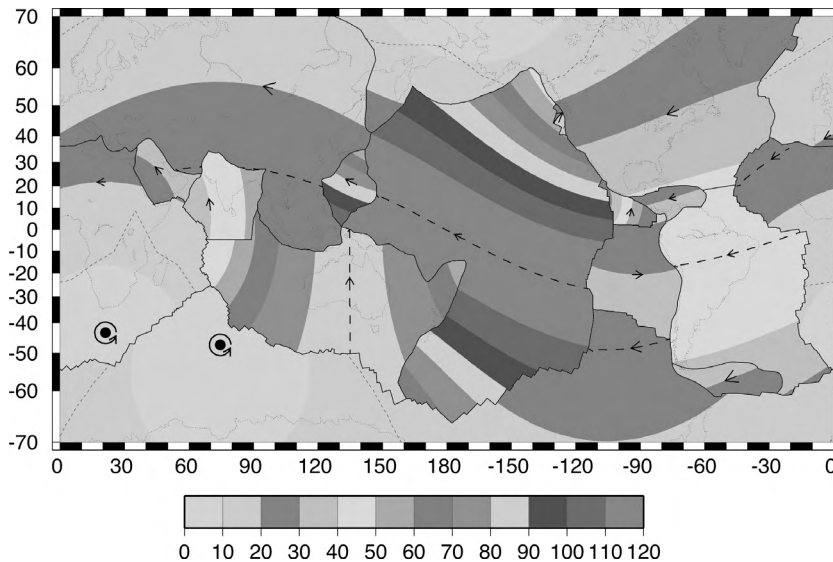
**Figure 2.19.** (a) The global distribution of hotspots (grey squares) and associated volcanic tracks. (After Norton, I. O. Global hotspot reference frames and plate motion. Geophysical Monograph 121, 339–57, 2000. Copyright 2000 American Geophysical Union. Reproduced by permission of American Geophysical Union.)



**Figure 2.19.** (b) Four volcanic island chains in the Pacific Ocean. The youngest active volcano is at the southeast end of each chain. (From Dalrymple *et al.* (1973).)



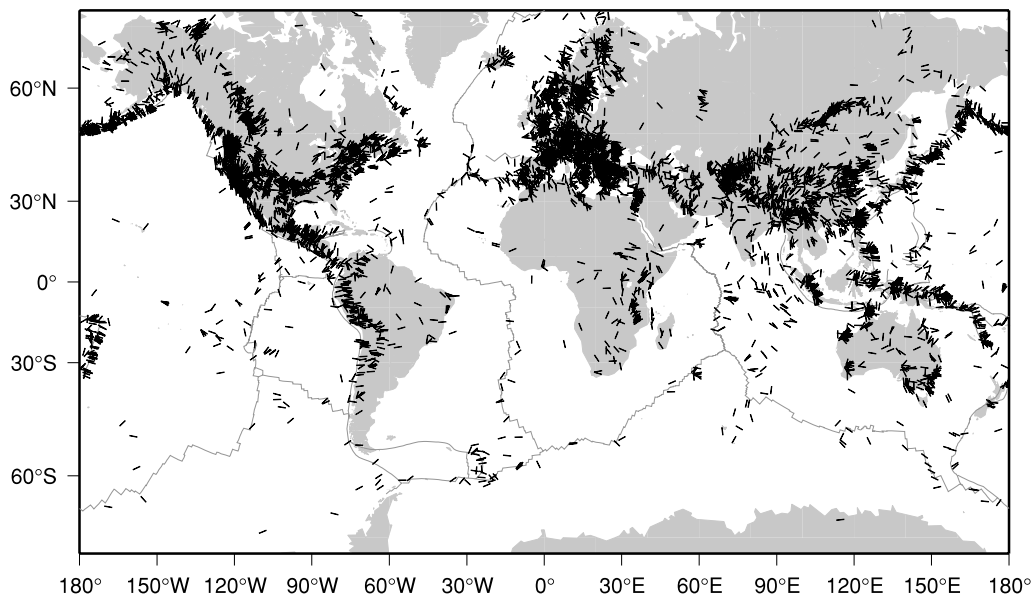
**Figure 2.19.** (c) A demonstration of the relative motions between the hotspot (fixed in the mantle) and the seamount chain on the overriding plate. The pencil represents the hotspot, which is fixed in the mantle (rectangular grid). The plate moves over the mantle and the pencil marks the line of seamounts (the 'hotspot track'). The star is the position of a seamount. After formation of the seamount, the plate moves north for one unit and then west for one unit so leaving a solid (pencil) line of seamounts, the hotspot track. The 'flow-line', the relative motion of the plate with respect to the hotspot, is the dashed line. (Reprinted with permission from *Nature* (Stein *Nature* 387, 345–6) Copyright 1997 Macmillan Magazines Ltd.)



**Figure 2.20.** Absolute motions of the plates as determined from hotspot traces. HS3-NUVEL-1A is a set of angular velocities of fifteen plates relative to the hotspots. The hotspot dataset HS3 averages plate motion over the last 5.8 Ma. No hotspots are in significant relative motion. The 95% confidence limit is  $\pm 20\text{--}40 \text{ km/Ma}^{-1}$  but can be  $145 \text{ km/Ma}^{-1}$ . (See Plate 1 for colour version). (From Gripp and Gordon (2002).)

The hotspot reference frame therefore is the motions of the plates relative to the hotspots, which are assumed to be fixed in the mantle. The ‘hotspot track’, the linear chain of volcanic islands and seamounts, is the path of the hotspot with respect to the overlying plate. The slow steady motion of the oceanic plate with respect to the hotspot (the flowline) is not marked by any feature, however. Figure 2.19(c) illustrates the difference between the hotspot track and the flowline. In order to use probable hotspot tracks to run the plate motions backwards, it is necessary to know the ages of the islands and seamounts, as we do for the Hawaiian chain. However, even if the ages of seamounts are unknown, the flow-lines can be used. By assigning a range of possible ages to any seamount, a series of flow-lines can be plotted (these will all follow the actual flow-line), producing a line that will go through the present position of the hotspot. (For example, when the seamount in Fig. 2.19(c) is erroneously assumed to be one unit old rather than two, the black dot shows the backtracked hotspot location – this lies on the flow-line but not on the hotspot track.) The process is then repeated for another seamount and the two sets of flow-lines compared. If the two seamounts formed at the same hotspot then the flow-lines will intersect at the location of that hotspot. If the seamounts were not formed by the same hotspot, the flow-lines should not intersect. Application of this method is improving our knowledge of hotspot locations and absolute plate motions.

Figure 2.20 shows a determination of the present absolute plate motions. Plate motions relative to hotspots cannot be estimated as accurately as can relative



**Figure 2.21.** A generalised world stress map. Lines show the orientation of the maximum horizontal stress. A colour version of the map showing the tectonic regimes – normal faulting, strike-slip faulting and thrust faulting – is available on-line. (From Reinecker *et al.* 2003, available on-line at <http://www.world-stress.org>.)

plate motions. This is because hotspot tracks have average widths in excess of 100 km, which is orders of magnitude greater than the width of active transform faults ( $<2$  km) and the width of the transition between magnetic anomalies (1–5 km). Continental plates tend to move more slowly than oceanic plates. Similarly, plates with more than a quarter of their perimeter subducting tend to move faster than plates that are hardly subducting anywhere. Values for the absolute motions obtained by different authors vary somewhat depending upon assumptions made and the particular relative plate motions used. Sources of uncertainty in determining absolute motions are the determination of the motions of the hotspot traces and assumptions about mantle dynamics and forces driving the plates. Nevertheless, a framework of motion can be developed even if some uncertainties remain. The Pacific and Indian plates are moving fast and the North American plate more slowly, while the Eurasian and African plates are hardly moving at all.

Figure 2.21 is a plot of the orientation of horizontal stress measured in the interior of the plates. The pattern of these intraplate stresses in the crust (stress is force per unit area) can be used to assess the forces acting on the plates. The direction of the stresses is correlated with the direction of the absolute plate motions (Fig. 2.20). This implies that the forces moving the plates around, which act along the edges of the plates (Section 7.10) are, to first order, responsible for the stresses in the lithosphere.



## Problems

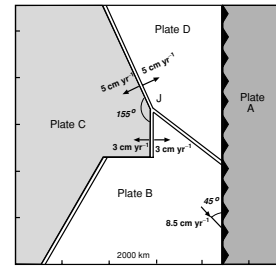
1. All plates A–D shown in Fig. 2.22 move rigidly without rotation. All ridges add at equal rates to the plates on either side of them; the rates given on the diagram are half the plate-separation rates. The trench forming the boundary of plate A does not consume A.

Use the plate velocities and directions to determine by graphical means or otherwise (a) the relative motion between plates B and D and (b) the relative motion between the triple junction J and plate A. Where and when will J reach the trench? Draw a sketch of the geometry after this collision showing the relative velocity vectors and discuss the subsequent evolution. (From Cambridge University Natural Sciences Tripos 1B, 1982.)

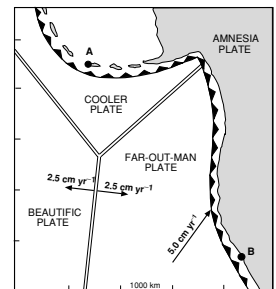
2. Long ago and far away in a distant galaxy lived two tribes on a *flat* planet known as Emit-on (Fig. 2.23). The tribe of the dark forces lived on the islands in the cold parts of the planet near A, and a happy light-hearted people lived on the sunny beaches near B. Both required a constant supply of fresh andesite to survive and collected the shrimp-like animals that prospered near young magnetic-anomaly patterns, for their food. Using the map and your knowledge of any other galaxy, predict the future of these tribes. (From Cambridge University Natural Sciences Tripos 1B, 1980.)
3. Use the map in Fig. 2.2 to do the following.

- (a) Calculate the relative present-day motions at the tabulated locations, using or calculating the appropriate poles from those given in Table 2.1.
- (b) Plot the azimuth and magnitude of these relative motions on the map.
- (c) Plot the pole positions. Note how the relative motions change along plate boundaries as the angular distance from the pole changes.
- (d) Discuss the nature of the plate boundary between the Indian/Australian and Pacific plates.
- (e) Discuss the nature of the plate boundary between the Eurasian and African plates between the Azores and Gibraltar. How does this boundary differ in the Mediterranean?

(From G. C. P. King, personal communication.)



**Figure 2.22.** A map of part of a flat planet.

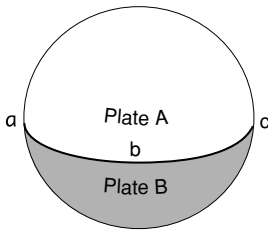


**Figure 2.23.** A map of part of Emit-on.

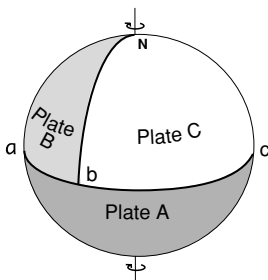
Latitude	Longitude	Location
54°N	169°E	W. Aleutian Trench
52°N	169°W	E. Aleutian Trench
38°N	122°W	San Francisco–San Andreas Fault
26°N	110°W	Gulf of California
13°S	112°W	East Pacific Rise
36°S	110°W	East Pacific Rise
59°S	150°W	Antarctic–Pacific Ridge
45°S	169°E	S. New Zealand
55°S	159°E	Macquarrie Island
52°S	140°E	Southeast Indian Ridge

(cont.)

Latitude	Longitude	Location
28°S	74°E	Southeast Indian Ridge
7°N	60°E	Carlsberg Ridge
22°N	38°E	Red Sea
55°S	5°E	Southwest Indian Ridge
52°S	5°E	Mid-Atlantic Ridge
9°N	40°W	Mid-Atlantic Ridge
35°N	35°W	Mid-Atlantic Ridge
66°N	18°W	Iceland
36°N	8°W	Gorringe Bank
35°N	25°E	E. Mediterranean
12°S	120°E	Java Trench
35°N	72°E	Himalayas
35°S	74°W	S. Chile Trench
4°S	82°W	N. Peru Trench
20°N	106°W	Middle America Trench



**Figure 2.24.** Planet Ares has just two plates.



**Figure 2.25.** Tritetkon has three plates.

- Define the pole of relative angular velocity for two plates and explain why it is a useful concept. Give two practical methods for finding poles of rotation from geophysical data. When these data are not available, how would you try to locate the poles? (Cambridge University Natural Sciences Tripos IB, 1977.)
- Ares is a planet with just two plates, A and B (Fig. 2.24). Plate B comprises the lower hemisphere and plate A the upper, as shown. Points a, b and c lie on the equator, and point d is diametrically opposite b. The zero meridian passes through point a. The pole of rotation of plate A relative to plate B is at 45°N, 0°E. The amplitude of the angular velocity vector is  $10^{-10}$  radians per terrestrial year. The radius of Ares is 3400 km.
  - What is the nature of the plate boundary between plates A and B?
  - State where magnetic lineations might be found and sketch the pattern that would be observed.
  - Calculate the relative velocity between plates A and B at locations a, b, c and d.
  - Sketch possible fault-plane solutions for earthquakes occurring at locations a, b, c and d.
  - Discuss the possible existence of such a two-plate planet.
  - Discuss briefly how the stability or instability of a two-plate tectonic system depends upon the pole position and/or relative size of the two plates.
- The lithosphere of Tritetkon, a recently discovered spherical satellite of Jupiter, consists of three plates, as shown in Fig. 2.25. Plate A is a hemisphere, and plates B and C are half a hemisphere each. Points a, b and c lie on its equator, and point d (not visible) lies diametrically opposite b. The zero meridian lies midway between b and d and passes through a. The pole of rotation B to A lies in plate B at latitude 30°N longitude 0°. The amplitude of the angular velocity vector through this pole is  $3 \times 10^{-9}$  radians per terrestrial year. The rotation pole C to B is at the north pole N, and the amplitude of the angular velocity vector is  $6 \times 10^{-9}$  rad yr<sup>-1</sup>. The radius of Tritetkon is 6000 km.

- (a) Find the coordinates of the angular velocity vector of C to A and its amplitude.
- (b) Draw velocity triangles for the triple junctions at b and d.
- (c) Tritecton has a magnetic field that reverses every ten million years. Draw the magnetic pattern created at the triple junction where extension is taking place. State whether it is at b or d.
- (d) The features at each plate boundary are trenches, transform faults or spreading ridges. Describe their distribution along each plate boundary.

(Cambridge University Natural Sciences Tripos IB, 1979.)

7. In Fig. 2.26, the trench between B and C is consuming B only. The ridge between A and B is spreading symmetrically at right angles to its axis. The pole of rotation between A and C is fixed to C. The angular velocity of A with respect to C is in the direction shown, and is  $2 \times 10^{-8} \text{ rad yr}^{-1}$  in magnitude.

- (a) Mark the poles of rotation and angular velocities of (i) plate B and (ii) the ridge axis with respect to plate C. (Remember that the pole of motion between two plates is that point which is stationary with respect to both of them.)
- (b) Show the direction and rate of consumption at X and Y.
- (c) How long will it take for the ridge to reach (i) X and (ii) Y?

Sketch the history of the triple junction between A, B and C with respect to C.

(Cambridge University Natural Sciences Tripos 1B, 1981.)

8. The three plates A, B and C meet at a ridge–ridge–ridge triple junction as shown in Fig. 2.27. The ridge between plates A and B has a half-spreading rate of  $2 \text{ cm yr}^{-1}$ . Calculate

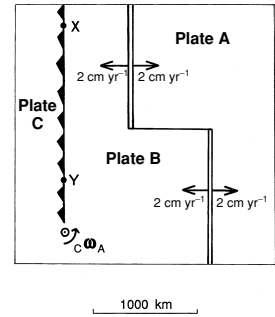
- (a) the half-spreading rates of the other two ridges and
- (b) the motion of the triple junction relative to plate C.

9. All the plates of Problem 1 move rigidly without rotation. Discuss the difference between those motions and the motions that would take place were the plates on the surface of a spherical Earth. (For example, by how much would the plate-separation rates vary along the length of the ridge between plates B and C?)

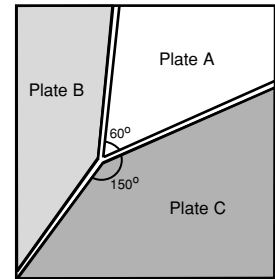
10. Four flat plates are moving rigidly, without rotation, on a flat Earth as illustrated in Fig. 2.28.

- (a) Determine the relative motion vector of the Beautific-Joker's–Nasty (BJN) triple junction to the Albatross plate.
- (b) Determine the relative motion vector of the Beautific-Nasty–Erratic (BNE) triple junction to the Albatross Plate.
- (c) Using these vectors, draw the loci of the future positions of these junctions relative to the Albatross plate. Mark points at 10-Ma intervals.
- (d) At 10-Ma intervals redraw the positions of the plate boundaries until both the Joker's plate and the Nasty plate have been consumed at the subduction zone boundary by the Albatross plate.
- (e) Draw velocity triangles for the triple junctions at the times when they pass through points A and B.
- (f) Draw the magnetic-anomaly pattern formed by the BJN junction for 10 Ma, assuming that a recognizable anomaly appears at 2-Ma intervals.

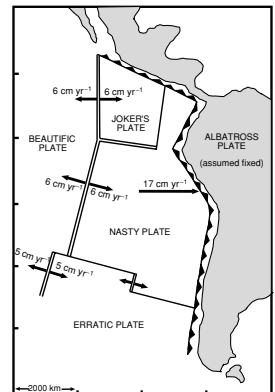
(From G. C. P. King, personal communication.)



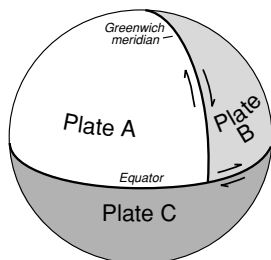
**Figure 2.26.** The map for Problem 7.



**Figure 2.27.** A ridge–ridge–ridge (RRR) triple junction.



**Figure 2.28.** Plates on a flat Earth.



**Figure 2.29.** A mythical planet has three plates.

11. Figure 2.29 depicts a mythical planet whose tectonic features comprise three plates A, B and C with boundaries as shown. The plate boundary A–B is a fault with sense of motion as shown and relative velocity of  $4 \text{ cm yr}^{-1}$ , and that between B and C is also a fault, with velocity  $3 \text{ cm yr}^{-1}$ .
  - (a) Using angular velocity vectors, find the pole of relative motion between plates A and C, giving its geographic coordinates. Calculate the relative angular velocity in degrees per year (the radius of the mythical planet is  $6000 \text{ km}$ ).
  - (b) Describe the tectonic nature of the boundary between plates A and C. Give details of places where magnetic lineations might be found (the mythical planet has a reversing magnetic field like the Earth's), what the maximum spreading rate might be expected to be, and any other geological and geophysical information you can deduce.
  - (c) Consider the triple junction where plates A, B and C all meet on the visible side of the mythical planet. What will happen to the triple junction if this instantaneous velocity description continues for several million years? In particular, think about the way ridges spread symmetrically and trenches consume on only one side. Is the junction likely to persist as drawn? What about the junction on the other side of the mythical planet? Is it similar?

## References and bibliography

- Altman, S. L. 1986. *Rotations, Quaternions and Double Groups*. New York: Oxford University Press.
- Argus, D. and Gordon, R. 1991. No-net rotation model of current plate velocities incorporating plate motion model NUVEL.1. *Geophys. Res. Lett.*, **18**, 2039–42.
- Barazangi, M. and Dorman, J. 1969. World seismicity maps compiled from ESSA Coast and Geodetic Survey, epicenter data, 1961–1967. *Bull. Seism. Soc. Am.*, **59**, 369–80.
- Båth, M. 1979. *Introduction to Seismology*, 2nd edn. Boston: Birkhauser.
- Bullard, E. C., Everett, J. E. and Smith, A. G. 1965. Fit of continents around the Atlantic. In P. M. S. Blackett, E. C. Bullard and S. K. Runcorn, eds., *A Symposium on Continental Drift*, *Roy. Soc. London, Phil. Trans. Ser. A*, **258**, 41–75.
- Carter, W. E. and Robertson, D. S. 1986. Studying the Earth by very-long-baseline-interferometry. *Sci. Am.*, **255**, 46–54.
- Chase, C. G. 1978. Plate kinematics: the Americas, East Africa and the rest of the world. *Earth Planet. Sci. Lett.*, **37**, 355–68.
- Chu, D. H. and Gordon, R. G. 1999. Evidence for motion between Nubia and Somalia along the southwest Indian ridge. *Nature*, **398**, 64–7.
- Coode, A. M. 1965. A note on oceanic transcurrent faults. *Can. J. Earth Sci.*, **2**, 400–1.
- Cox, A., ed. 1973. *Plate Tectonics and Geomagnetic Reversals*. San Francisco, California: Freeman.
- Cox, A. and Hart, R. B. 1986. *Plate Tectonics: How it Works*. Oxford: Blackwell Scientific.
- Dalrymple, G. B., Silver, E. A. and Jackson, E. D. 1973. Origin of the Hawaiian islands. *Am. Scientist*, **61**, 294–308.
- DeMets, C., Gordon, R. G., Argus, D. F. and Stein, S. 1990. Current plate motions. *Geophys. J. Int.*, **101**, 425–78.

1994. Effects of recent revisions to the geomagnetic reversal time scale on estimates of current plate motions. *Geophys. Res. Lett.*, **21**, 2191–4.
- Dickinson, W. R. and Snyder, W. S. 1979. Geometry of triple junctions related to San Andreas transform. *J. Geophys. Res.*, **84**, 561–72.
- Gordon, R. G. and Jurdy, D. M. 1986. Cenozoic global plate motions. *J. Geophys. Res.*, **91**, 12 389–406.
- Gripp, A. E. and Gordon, R. G. 1990. Current plate velocities relative to the hotspots incorporating the NUVEL-1 global plate motion. *Geophys. Res. Lett.*, **17**, 1109–12.
2002. Young tracks of hotspots and current plate velocities. *Geophys. J. Int.* **150**, 321–61.
- Gubbins, D. 1990. *Seismology and Plate Tectonics*. Cambridge: Cambridge University Press.
- Harper, J. F. 1986. Mantle flow and plate motions. *Geophys. J. Roy. Astr. Soc.*, **87**, 155–71.
- Irving, E. 1977. Drift of the major continental blocks since the Devonian. *Nature*, **270**, 304–9.
- Kroger, P. M., Lyzenga, G. A., Wallace, K. S. and Davidson, J. M. 1987. Tectonic motion in western United States inferred from very long baseline interferometry measurements, 1980–1986. *J. Geophys. Res.*, **92**, 14 151–63.
- Larson, K. M., Freymueller, J. T. and Philipson, S. 1997. Global plate velocities from the Global Positioning System. *J. Geophys. Res.*, **102**, 9961–81.
- Le Pichon, X., Francheteau, J. and Bonnin, J. 1973. *Plate Tectonics*. Vol. 6 of Developments in Geotectonics. Amsterdam: Elsevier.
- Lowman, P. D. 1992. Geophysics from orbit: the unexpected surprise, *Endeavour*, **16**, (2), 50–8.
- McKenzie, D. P. and Morgan, W. J. 1969. Evolution of triple junctions. *Nature*, **224**, 125–33.
- McKenzie, D. P. and Parker, R. L. 1967. The north Pacific: an example of tectonics on a sphere. *Nature*, **216**, 1276–80.
- Minster, J. B. and Jordan, T. H. 1978. Present-day plate motions. *J. Geophys. Res.*, **83**, 5331–54.
- Molnar, P. and Stock, J. 1987. Relative motions of hotspots in the Pacific, Atlantic and Indian Oceans since Late Cretaceous time. *Nature*, **327**, 587–91.
- Morgan, W. J. 1968. Rises, trenches, great faults and crustal blocks. *J. Geophys. Res.*, **73**, 1959–82.
1971. Convection plumes in the lower mantle. *Nature*, **230**, 42–3.
- Norton, I. O. 2000. Global hotspot reference frames and plate motion. In M. A. Richards, R. G. Gordon and R. D. van der Hilst, eds., *The History and Dynamics of Global Plate Motions*. Geophysical Monograph 121. Washington: American Geophysical Union, pp. 339–57.
- Reinecker, J., Heidbach, O. and Müller, B. 2003. The 2003 release of the World Stress Map (<http://www.world-stress.org>).
- Royer, J.-Y. and Gordon, R. G. 1997. The motion and boundary between the Capricorn and Antarctic plates. *Science*, **277**, 1268–74.
- Shen *et al.* 1997. Crustal deformation measured in southern California. *EOS Trans. Am. Geophys. Un.*, **78** (43), 477 and 482.
- Stein, R. S. 1987. Contemporary plate motion and crustal deformation. *Rev. Geophys.*, **25**, 855–63.
1988. Plate tectonic prediction fulfilled. *Phys. Today* (January), S42–4.
- Stein, S. A. 1997. Hot-spotting in the Pacific. *Nature*, **387**, 345–6.

- Steinberger, B., Sutherland, R. and O'Connell, R. J. 2004. Prediction of Emperor-Hawaii seamount locations from a revised model of global plate motion and mantle flow. *Nature*, **430**, 167–73.
- Stella, G. F., Dixon, T. H. and Mao, A. 2002. REVEL: a model for recent plate velocities from space geodesy. *J. Geophys. Res.* **107** (B4), doi: 10.1029/2000JB000033.
- Sykes, L. R. 1967. Mechanism of earthquakes and nature of faulting on the mid-ocean ridges. *J. Geophys. Res.*, **72**, 2131–53.
- Wessel, P. and Kronke, L. 1997. A geometric technique for relocating hotspots and redefining absolute plate motions. *Nature*, **387**, 365–9.
- Wilson, J. T. 1965. A new class of faults and their bearing on continental drift. *Nature*, **207**, 343–7.
- Zatman, S., Gordon, R. G. and Richards, M. A. 2001. Analytic models for the dynamics of diffuse oceanic plate boundaries. *Geophys. J. Int.*, **145**, 145–56.
- Ziegler, A. M., Scotese, C. R., McKerrow, W. S., Johnson, M. E. and Bambach, R. K. 1979. Paleozoic paleogeography. *Ann. Rev. Earth Planet. Sci.*, **7**, 473–502.
- Zoback, M. L. 1992. First- and second-order patterns of stress in the lithosphere: the World Stress Map Project. *J. Geophys. Res.*, **97**, 11 703–28.
- Zoback, M. L. *et al.* 1989. Global patterns of tectonic stress: a status report on the World Stress Map Project of the International Lithosphere Program. *Nature*, **341**, 291–8.
- Zoback, M. D. and Zoback, L. M. 1991. Tectonic stress field of North America and relative plate motions. In D. B. Slemmons, E. R. Engdahl, M. D. Zoback and D. D. Blackwell, eds., *Neotectonics of North America*. Geological Society of America Decade Map Vol. 1. Boulder, Colorado: Geological Society of America, pp. 339–66.